An-Najah National University

Faculty of Graduate Studies

PREPARATION OF COPPER NANOPARTICLES ONTO COPPER SHEETS AND ELECTROCATALYTIC APPLICATION IN WATER DE-NITRATION

By

Samaa Masoud Asaad Hijazi

Supervisors

Prof. Hikmat Hilal

Dr. Heba Nassar

This Thesis is Submitted in Partial Fulfillment of the Requirements for The Degree of Master of Chemistry, Faculty of Graduate Studies, An Najah National University, Nablus-Palestine.

2024

PREPARATION OF COPPER NANOPARTICLES ONTO COPPER SHEETS AND ELECTROCATALYTIC APPLICATION IN WATER DE-NITRATION

By
Samaa Masoud Asaad Hijazi

This thesis was Defended successfully on 01/04/2024, and approved by:

Prof. Hikmat Hilal Supervisor	Signature
Dr. Heba Nassar Co-Supervisor	Signature
Prof. Sameer Bsharat External Examiner	Signature
Prof. Shehdeh Jodeh Internal Examiner	Signature

Dedication

To the spirit of all the fearless Palestinian martyrs who laid down their lives to light our path to freedom.

To Palestine.

To my Beloved Family.

In memory of Mansour and Asaad.

To my dear Sina and Durgham, without whom the voyage would have been impossible.

And finally, to you, my dear reader…

Acknowledgement

After praising Allah, who enabled me to complete what I had begun. My deepest gratitude goes to Prof. Hikmat Hilal, my most important advisor, for all of his help, guidance, and insight during this entire endeavor. Dr. Heba Nassar, my research co-supervisor, who never left my side throughout all my research stages, deserves a great deal of gratitude for her unending support, wisdom, and advice. Please accept my sincere appreciation for Dr. Derar Alsmadi and the rest of the chemistry faculty at An-Najah National University.

Acknowledgments are extended to Mr. Ameed Amera and Mr. Nafith Dweikat, members of the laboratory technical team, for their valuable contributions. I would also want to express my gratitude to Professor Tae Woo Kim and his research team from the Korean Institute of Energy Research in Daejeon, South Korea, for conducting scanning electron microscopy (SEM), energy-dispersive X-ray spectroscopy (EDS), X-ray diffraction (XRD), and X-ray photoelectron spectroscopy (XPS) analyses.

Finally, I'd like to express my unending gratitude to my father, mother, sisters, and brothers for believing in me and supporting me no matter what as I pursued my education.

Finally, I would like to express my gratitude to my fiancé Abdelrahman, for his unwavering support and encouragement.

Samaa Hijazi

Declaration

I, the undersigned, declare that I submitted the thesis entitled:

PREPARATION OF COPPER NANOPARTICLES ONTO COPPER SHEETS AND ELECTROCATALYTIC APPLICATION IN WATER DE-NITRATION

Unless otherwise referenced, I declare that the work provided in this thesis is the researcher's work and has not been submitted elsewhere for any other degree or qualification.

Student's Name: سماء محمود أنور حجازي

Signature: Samaa

Date: ٢٠٢٢/٤/١

List of Contents

List of Tables

List of Figures

List of Appendixes

PREPARATION OF COPPER NANOPARTICLES ONTO COPPER SHEETS AND ELECTROCATALYTIC APPLICATION IN WATER DE-NITRATION

By
Samaa Masoud Asaad Hijazi
Supervisors
Prof. Hikmat Hilal
Dr. Heba Nassar

Abstract

The issue of water contamination, specifically with nitrate ions, is a growing concern on global and Palestinian levels. This pertains to both groundwater and surface water sources. The escalation in nitrate pollution can be attributed to the excessive and improper utilization of chemicals as a consequence of human activities. The utilization of electrochemical reduction of nitrate presents a viable method for addressing this issue. The key goal of this study is to enhance the removal of nitrate by highly selective electroreduction to N_2. The aforementioned objective is accomplished through the alteration of an inexpensive, reliable, and durable electrode that exhibits exceptional efficiency in nitrate reduction. The bench-scale undivided electrochemical cell was utilized in the potentiostatic mode, aiming to obtain reduced power consumption. The experimental setup consisted of three distinct electrodes: a reference electrode known as the saturated calomel electrode (SCE), a counter electrode in the form of a platinum (Pt) sheet, and one of the newly modified electrodes served as the working electrode. Customized electrodes comprise Cu@Cu modified by electrodeposition of Cu nanoparticles on a chemically pure Cu sheet, $FeCl_3$ chemically etched copper electrodes, and copper sheets modified by graphene. The graphene modification was eliminated due to several reasons that will be discussed later. The electrodes underwent characterization through the utilization of X-ray diffraction (XRD), scanning electron microscopy (SEM), energy-dispersive X-ray spectroscopy (EDS), and X-ray photoelectron spectroscopy (XPS). Among the studied electrodes, the copper nanoparticle electrodeposited electrode (Cu@Cu-1) results displayed the most significant nitrate conversion rate, reaching 92.3% and 85.05% selectivity towards N_2 gas within a time frame of 420 minutes. Furthermore, the kinetics associated with the electrochemical reduction of nitrate via the Cu@Cu-1 electrode was examined through the use of the initial rate method. The investigation revealed a reaction rate order of

0.85. Additionally, the rate constant was determined by analyzing the intercept of the plot that is equal to ln k, from which k was found to = 1.39×10^{-2} min^{-1}.

Keywords: Copper Nanoparticles; Copper; Electrochemical reduction; Nitrate ions; Water Pollution,

Chapter One

Introduction and Literature Review

1.1 General Background and Problem Statement

Water is one of the most important aspects of humans' availability and development on Earth. Water levels on earth are almost constant, approximated at the height of $1600 \times 106\ km$ (1). Although most of the earth's surface isn't land but is in fact covered in water, not all the available water is directly valid for individuals (2). Seawater corresponds to 97.2% of the overall volume and is unserviceable for human needs, an additional 2.1% is denoted for ice and snow, leaving out 0.6% of the total water capacity as fresh, usable water (1). Groundwater is estimated to compose 98 percent of the total freshwater reserves and is the most copious source (3). Approximately one-half of the global population relies on groundwater as their primary source of drinking water. Not only is it the main source of drinkable fresh water, but it's also fundamental in many other aspects regarding every form of life and the well-being of the earth; it helps sustain the ecosystem and maintains a stable temperature (4). Humans' uses of groundwater may vary depending on the situation, it can be used in food production, agriculture, energy production, etc. For these reasons, groundwater is an essential factor in human progress. Since groundwater is a readily accessible source that mostly requires little or no treatment, it is globally preferred by beings for survival over surface water as a supply of fresh, usable water (3,4).

In recent years, water scarcity is no longer the only concern regarding water. With industrialization development and population growth, a stumbling block has occurred and it's the quality of the water (5). The statement quality of water conveys the chemical, biological, and physical features of the water (6). The quality of water has become a major threat due to pollution caused by the significant increase in the concentration of uncommon substances and natural components (3,6). Hence, pollution is an outcome of human activity and genuine incidents by nature (6). As stated, earlier contamination of groundwater resources is anthropogenic or natural, anthropogenic is due to diverse actions that generally involve (3–6):

- Agriculture activities,
- Mistreatment of chemicals,

- Discarding wastewater, and solid waste,
- Discarding industrially contaminated water,
- Etc.

Moreover, although human activities are the most abundant reason for world pollution, they aren't the only reason for groundwater contamination, groundwater may also get polluted via natural motives, as an outcome of natural occurrences, or cycles. The natural causes category consists of (1,3,5,6):

- Chemical reactions in water,
- Radioisotopes decay from the uranium-rich substratum,
- Extreme evaporation,
- Easily dissolved rocks,
- Etc.

As a result of water resources contamination, elements such as (Ni, Se, B, Cr, Cu, Al, Fe, etc.) were detected in high concentrations in groundwater mines (1). Other impurities detected in groundwater that are also linked to human activities include hydrocarbons, nitrates, halogens, biphenyls, and biological impurities (6). Various health issues affecting living organisms have been linked to water pollution, for instance, Fluorosis, Diarrhea, Blackfoot, etc. are all waterborne infections (5).

Globally, nitrate has become one of the most predominant chemicals detected in groundwater, initiated by an array of practices associated with agriculture, industry, and other similar practices (7). The elevated levels of nitrate in drinking water in recent years have caused significant public concern due to the potential for severe health issues; it may lead to methemoglobinemia in toddlers and abdominal cancer in grownups (8). Therefore, nitrate contamination is a critical matter, and efforts should be made to resolve it and find appropriate ways for denitrification to attain sustainable sources of fresh and safe drinkable water.

1.2 The Nitrogen Cycle and Imbalance

The majority of Earth's atmosphere is composed of nitrogen; nitrogen (N) is considered to be the fourth most abundant element in cellular biomass (9). The major nitrogen reserve on planet earth is the triple-bonded N_2 gas (78% of the total atmosphere). Nitrogen may exist in many different chemical formulas, several oxidations, and reduction state (10). For nitrogen to be useful in human activities, it should be in the form of inorganic compounds (11). There is no doubt that the nitrogen cycle takes second place among the most essential cycles after the carbon cycle (11). The nitrogen cycle is the alteration of different nitrogen forms generated by two major processes: biological and physical processes that are dependent on a range of environmental aspects that affect its availability (11). The nitrogen cycle was simplified and separated into four major procedures listed as follows (9):

1. Fixation,
2. Nitrification,
3. Oxidation,
4. Denitrification.

A basic representation of the major nitrogen cycle processes was developed and presented in Figure 1.1.

Figure 1.1

Basic Nitrogen Cycle Scheme

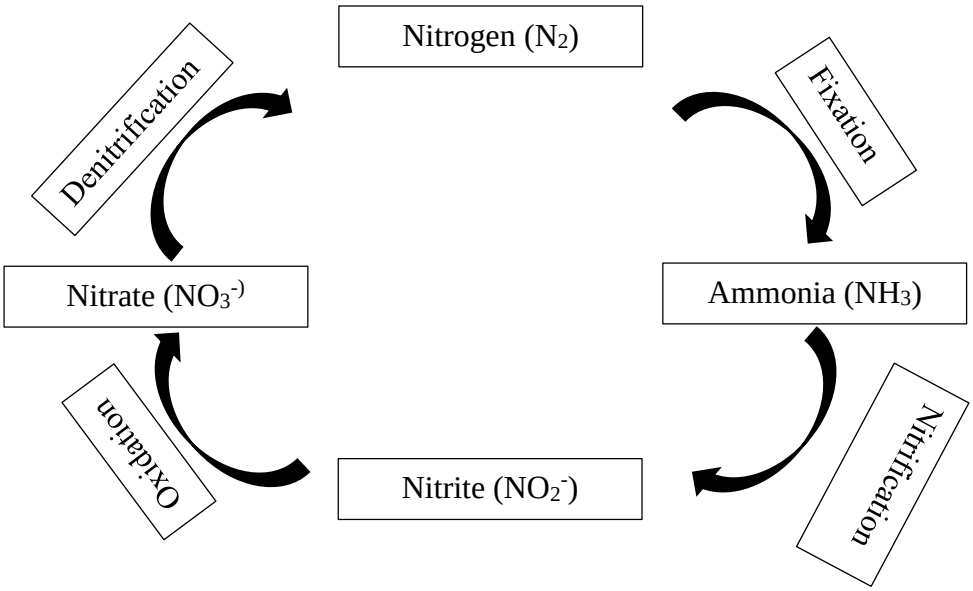

In order for dinitrogen to be of use in human activities, it should be readily available by means of inorganic compounds such as nitrate, nitrite, ammonia, or ammonium (11). Nitrogen fixation comes as the first step in the nitrogen cycle, and it's the way atmospheric N_2 is converted into ammonia (NH_3) or ammonium (NH_4^+) according to equation 1.1, (12). Fixation of nitrogen is achieved by nitrogen-fixing bacteria (Azotobacter, Rhizobium, Clostridium, etc.) located in the roots of specific plants or in soil. These different types of bacteria convert N_2 into ammonia and ammonium to be easily converted into other various nutrients (9,12–14).

$$N_2 + 8H^+ + 8e^- \rightarrow 2NH_3 + H_2 \quad \text{(1.1)}$$

The second step in the cycle is nitrification, which is a process carried out by ammonia-oxidizing bacteria that converts ammonia to nitrite according to equation 1.2, *Nitrosomonas* is the main type of bacteria associated with this step, although there are several other genera that are associated with the nitrification of ammonia (15,16).

$$NH_3 + O_2 \rightarrow NO_2^- + 3H^+ + 2e^- \quad \text{(1.2)}$$

As the cycle goes on, the third step in the cycle is oxidization. Nitrite-oxidizing bacteria oxidize nitrite to nitrate, as equation 1.3 states. *Nitrobacter* is the identified type in this process, along with other genera that also have the ability to oxidize nitrate (15,16).

$$NO_2^- + H_2O \rightarrow NO_3^- + 2H^+ + 2e^- \quad \text{(1.3)}$$

Finally, the cycle ends with the denitrification process, which converts nitrate back into its primary form as atmospheric nitrogen (N_2). Denitrification is a procedure carried out by certain types of bacteria found in the soil, such as *Bacillus* and *Pseudomonas*, converting nitrate into nitrogen as stated in equation 1.4 and releasing it back to the atmosphere (16,17).

$$2NO_3^- + 10_e^- + 12H^+ \rightarrow N_2 + 6H_2O \quad \text{(1.4)}$$

Human activities have significantly perturbed the nitrogen cycle and disrupted its equilibrium, resulting in an imbalance. The present management of nitrogen derivatives in water is regarded as one of the numerous critical challenges facing humankind in the 21^{st} century (18,19). Contamination of different water resources (Surface water or groundwater) with various pollutants especially nitrate-related pollution, has become a

significant issue around the world specifically in underdeveloped areas, as a result, humans are exhibited to intake nitrate concentrations beyond the normalized limit (20). Therefore, the increase in nitrate contamination has several disadvantages regarding the environment and human health.

1.3 Environmental and Health Concerns

On a global scale, nitrate contamination is a developing concern for both public and environmental health, as it poses a major risk to all living things. As stated previously, nitrate is a naturally occurring compound that is used in many human activities and is found in different water resources. However, the unmonitored excessive use of nitrate and poor practices are leading to an increase in nitrate levels in the environment, which is leading to food crops and water source contamination (8).

In Palestine, particularly in the West Bank there has been an observed increase in nitrate content in groundwater aquifers, surpassing the maximum limit set by the World Health Organization of (50 mg/L) (21). This phenomenon is attributed to agricultural activities and other contributing factors (22). During the time span from 1982 to 2004, there was a significant rise in the content of nitrate, surpassing 100 mg/L in numerous locations and exceeding 200 mg/L in certain areas within the West Bank (22).

Water sources' contagion with nitrate may commence an array of environmental worries. For instance, when nitrate levels exceed natural levels in ***seawater***, its toxicity on aquatic animals increases since nitrate converts oxygen-transporting pigments to pigments that are incompetent to carry oxygen (ex: Hemoglobin is altered to methemoglobin) (23).

Then again, the effect of elevated concentrations of nitrate affected water quality and posed serious health risks for humans, specifically for infants less than 6 months old and pregnant women (19). Nitrite is a nitrate derivative that causes methemoglobinemia, or “blue baby syndrome,” which is an outcome of the interference with the oxygen-carrying capacity of red blood cells. These syndromes lead to reduced oxygen supply to vital organs and are life-threatening for infants (21).

Nitrate also poses health concerns for adults, while nitrate is non-toxic, it may be converted to nitrite after ingestion through microbial action in the gastrointestinal tract,

which may lead to nitrite reacting with amino acids to form nitrosamines that are carcinogens (24). Consumption of nitrate-contaminated water or nitrate-rich food is linked with an intensified risk of certain types of cancer, including colorectal and gastric cancer (25).

Consequently, it is necessary to conduct research and devise a method that effectively eliminates nitrates from water across a wide range of size scales.

1.4 Regulations and Recommendations

Nitrate in drinking water is the primary route of exposure for humans. The World Health Organization (WHO) has capped nitrate (expressed as NO_3^-) levels in surface as well as groundwater at 50 mg L^{-1} in an effort to reduce or preferably eliminate the adverse health consequences accompanied with nitrate contamination (26).

1.5 Competing Purification Technologies

The increase of nitrate levels in human consumable water led to severe health issues, and the rising issue of nitrate contamination forced scientists to research and discover nitrate removal methods. Numerous technologies were uncovered, developed, and employed in denitrification. The several approaches were typically categorized into physical, biological, and chemical denitrification technologies.

1.5.1 Physical Methods

It is important to note that physical nitrate removal methods solely focus on the separation of nitrates without any means of their destruction (27–30). Physical methods commonly employed for water treatment include reverse osmosis, electrodialysis, ionic exchange utilizing resins, as well as coagulation and flocculation techniques (27,28,31–33). The aforementioned techniques necessitate frequent regeneration and are widely acknowledged for their elevated costs and the production of concentrated nitrate effluents. Therefore, such methods aren’t very promising and need improvement before relying on them.

1.5.2 Biological Methods

The biological method has been widely acknowledged as a favorable choice in various studies (34,35). The current approach exhibits certain limitations. It is characterized by a relatively slow reaction rate, posing challenges in terms of control. In addition, the process generates organic residues, which may have implications for subsequent steps (27). Furthermore, it is vital to note that this approach is not suitable for concentrations exceeding 1000 mg L^{-1} of NO_3^- beyond this threshold, the elevated levels of nitrate can be toxic to the bacteria (27,35). The two major drawbacks of a broad implementation include the high initial investment costs and the inability to precisely monitor process parameters due to technical constraints (36).

1.5.3 Chemical Methods

Chemical reduction, often employing hydrogen gas as the reducing agent, poses certain challenges due to the inherent difficulties associated with handling this particular gas (37,38). This reduction process is typically facilitated by the presence of metal catalysts (27). The utilization of this particular methodology necessitates the utilization of substantial quantities of metallic elements and has the potential to generate undesired secondary substances in high concentrations, namely nitrite and ammonium (37,39).

1.5.4 Electrochemistry

Electrochemistry is a subfield of chemistry that examines chemical reactions involving electron transfer at the electrode-electrolyte interface field. The acquisition of electrons by a chemical species is referred to as reduction, which is a fundamental process in electrochemistry (40). Electrochemistry provides valuable insights into reduction reactions and plays an essential role in numerous applications, such as energy storage, chemical synthesis, and environmental remediation (40).

More importantly, although electrochemistry has numerous applications in several fields (41). Due to the nature of this research, it is critical to state and review the use of electrochemistry in environmental remediation. It provides an efficient method for removing and degrading pollutants from water, wastewater, and soil, such as heavy metals and organic contaminants (41). Through the application of an adequate voltage and the selection of electrode materials, electrochemical reduction procedures can convert toxic species into less dangerous or easily separable forms (41).

The electrochemical reduction technique to treat aqueous contaminated water with several hazardous materials, such as oxyhalides and oxynitrogen was first developed by Olin (42,43). It has lately obtained the researcher's attention and it has been employed to treat contaminated aqueous solutions such as urine, contaminated water resources, and wastewater (44–46). Since electrochemistry has proven its efficiency in the reduction of water contaminants, it may be employed to handle high nitrate concentrations with simple device arrangements. This approach resulted in several advantages: no sediment was generated, and no start-up time was necessary, reducing the high costs of treatment (46, 47).

Electrocatalysis entails the occurrence of reactions at the interface between the electrode and reactant. The reaction can be made better if there is more charge flow through the electrodes along with the electrolyte (48).

There are three mechanisms at work in the electrocatalytic reduction of nitrate (49):

1. Introduce electrocatalytically active ions into the solution of choice (50).
2. Inhibiting the metal catalyst on the cathode outer layer (51).
3. Electroreduction is effectively initiated on the solid-modified electrode (52, 53).

Electrolysis can proceed in either a potentiostatic or a galvanostatic mode, each of which represents a unique mode of operation (54). During the potentiostatic electrolysis mode, an ongoing electrically powered potential (E in V) is maintained between the three electrodes of the electrochemical cell, which consist of a working electrode (cathode), a reference electrode, and a counter electrode. Only relevant reactions can be carried out in this approach of experiment depending on the given potential and its probable adequacy (55). That said, due to thermodynamic reasons, nitrate reduction requires relatively greater potentials than ideally required potentials (over-potentials) (56). To overcome large activation energy, an overpotential is required (57). Due to the high activation energy, the nitrate reduction pace is less rapid than in the galvanostatic mode.

As mentioned above, the galvanostatic electrolysis mode may be more rapid in nitrate reduction. To carry out galvanostatic electrolysis, a steady flow of current (j in $mAcm^{-2}$) is passed between a pair of electrodes in a simple electrochemical cell. Industrial applications favor galvanostatic systems due to their simplicity of operation. Despite

that, the lack of a prospective reference control and competing reactions reduce the faradaic efficiency (40,58,59).

1.5.4.1 Nitrate Electrochemical Reduction

The success rate and the precision of denitrification by electrocatalysis are influenced by several factors, including the applied current, the electrode material, the amount of time, the temperature, and the pH of the electrolyte (60,61). The procedure is additionally affected by both the type and quantity of electrolytes in the nitrate solution (60, 62). Thus, different electrolytes have undergone research studies, particularly, sodium sulfate (Na_2SO_4) (63, 64), and sodium chloride (NaCl) (65).

It should be mentioned that the parameters for nitrate electroreduction do not have a consistent approach. The literature displays a variety of approaches, with unpredictable and contradictory outcomes and interpretations. Researchers don't agree on a single set of procedures after going over literature reviews. Therefore, it is essential to investigate the impact of the aforementioned dynamics on the experiment before developing a suitable nitrate electroreduction system.

When dealing with highly concentrated nitrate solutions, the possible reaction pace is determined by the ratio of available surface catalytic cavities on an electrode (66). In order to maximize nitrate uptake, it is required to enhance the electrode specific surface area (SSA) while simultaneously reducing the uptake of any competing anions. Thus, the primary aim of this research is to acquire an electrode with an extremely large surface area. In this study, we will examine these factors in depth to develop a nitrate electroreduction system that operates at peak efficiency. For the sake of comparison, there will also be an investigation of electrolysis carried out without any electrode modifications.

1.5.4.2 Theoretical Framework of Nitrate Electrochemical Reduction

The lowest 1unoccupied molecular orbital 1(LUMO*) for the nitrate ion has a comparatively elevated energy level, which contributes to the high activation energy and delayed nitrate reduction process. As a result, it takes time and effort to add an electrical charge to the nitrate ion LUMO. Considering the activation energy required, the cathode voltage must be sufficiently high to promote electron transfer (10, 55).

Copper (Cu), Silver (Ag), and Platinum (Pt) are metals with partially full or significantly occupied d-orbitals that could contribute to electrochemical nitrate reduction (10). This is dependent on the potential gap between the 1d-orbital 1energy levels of the metals 1and the 1LUMO levels of the nitrate ion (10).

1.5.4.3 Products and Intermediates of Nitrate Electroreduction

The production of nonhazardous nitrogen gas is the overriding aim of nitrate electrochemical reduction research (20). Nevertheless, ammonia and 1nitrate are two recurring byproducts, and this reduces the efficacy of electrochemical denitrification (20,67). There are several other infrequent byproducts that include NH_2OH, NO_2, NO, N_2O, and NH_2NH_2 (20). Below are the main reactions of the nitrate electroreduction process (68). Nitrate electroreduction might seem like an extensive process it is often defined by reactions No. (1.6 & 1.7) (69).

$$NO_3^- + H_2O + 2e^- \rightleftharpoons NO_2^- + 2OH^- \quad \text{(1.5)}$$

$$NO_3^- + 3H_2O + 5e^- \rightleftharpoons \frac{1}{2}N_2 + 6OH^- \quad \text{(1.6)}$$

$$NO_3^- + 6H_2O + 8e^- \rightleftharpoons NH_3 + 9OH^- \quad \text{(1.7)}$$

$$NO_2^- + 5H_2O + 6e^- \rightleftharpoons NH_3 + 7OH^- \quad \text{(1.8)}$$

$$NO_2^- + 4H_2O + 4e^- \rightleftharpoons NH_2OH + 5OH^- \quad \text{(1.9)}$$

$$2NO_2^- + 4H_2O + 6e^- \rightleftharpoons N_2 + 8OH^- \quad \text{(1.10)}$$

$$NO_2^- + H_2O + 2e^- \rightleftharpoons NO_2^- + 2OH^- \quad \text{(1.11)}$$

Denitrification is accomplished by the direct interaction between the cathode surface and nitrate, resulting in nitrogen gas along with hydroxyl ions (No. 1.6) (70).

1.5.4.4 Copper as a Catalyst

The transition metal copper (Cu) plays a crucial role in many electrochemical reactions, especially in catalyzing nitrate reduction, and so is significant to electrochemistry. To date, this metal has garnered considerable attention from researchers, leading to extensive studies aimed at understanding and developing its catalytic properties and potential applications in this specific domain (20). Copper, which is also the most

widely available and inexpensive option, has been widely acknowledged as the most reactive metal in this domain of work (69). Nevertheless, the utilization of copper cathodes in nitrate treatment is limited because of their inadequate stability, primarily due to issues related to corrosion and leaching in addition to their selectivity towards ammonia as a significant by-product (71). The forthcoming chapter will delve into a comprehensive analysis of various recent endeavors pertaining to the modification of electrodes for the purpose of nitrate electroreduction. Particular emphasis will be placed on the exploration of copper electrodes.

1.6 Literature Review

The most recent review of nitrate electrochemical reduction was conducted by Meng *et al.* in 2023 (72). Several reviews about nitrate electrochemical reduction were made, in 2010 a review was written by Haque and Tariq (73), and another review was also accomplished by Kaczur in 1998 (74). Conversely, the upcoming lines provide a critical overview of contemporary literature on the alteration of electrodes, with a specific focus on the electroreduction of nitrate, particularly in relation to the copper cathode.

1.6.1 Categorization of Cathode Materials for Nitrate Electroreduction

Efforts were undertaken to fabricate electrodes with different materials for nitrate electroreduction. The objective was to enhance N_2 selectivity while minimizing the energy expenditure associated with the reaction (20). Several materials have been investigated in previous studies, including noble metals such as palladium (Pd) (75), and platinum (Pt) (38,66,76,77) in spite of their high efficiency in nitrate reduction, the necessity for alternate materials arises as a result of their exorbitant cost and limited availability. Other alternative materials were examined, such as lead (Pb) (49), nickel (Ni) (76), titanium (Ti) (65), zinc (Zn) (78), aluminum (Al) (79), silver (Ag) (80), iron (Fe) (39) and copper (Cu) (69,80).

However, copper has been identified as the most operational electrocatalyst 1for the electroreduction of aqueous NO_3^- with NH_4^+ as the ultimate product (69).

1.6.1.1 Copper and Associated Electrodes

The Cu metal electrode was investigated by many researchers for nitrate electroreduction (81–83), where ammonia was mainly yielded as a product of the procedure catalyzed by Cu (49,53). The electrocatalytic behavior of a pure copper cathode has been explored for (0.1 M $NO_3^{-)}$ in (1 M NaOH) "alkaline conditions" by Reyter *et al.* (69). The research revealed that the electroreduction of nitrate to nitrite on the copper electrode was the rate-determining phase in the reduction process.

1.6.1.2 Bimetallic Copper Electrodes

In order to enhance the efficiency of the copper electrode, many metals were employed for its modification, including Cu/Pt (84), Cu/Pd (85), Cu/Ni (86), Cu/Zn (87), Cu/MWCNT/FTO (88) electrode, and several more.

1.6.1.3 Cu/Pt Electrode

In 2017, two forms of platinum nanoparticles (NP) were investigated by Ehrenburg *et al.* (84). Polyoriented and cubic platinum nanoparticles, both NPs were accommodated on glassy carbon followed by a coat of Cu adatoms. Kinetics and mechanisms were studied by cyclic voltammetry (CV). It was revealed that the deposition of a copper adlayer on platinum nanoparticles resulted in increased stability and enhanced nitrate reduction kinetics.

1.6.1.4 Cu/Pd Electrode

The reduction of nitrate in basic solutions was investigated using dense, porous Cu-Pd alloy films. Porous electrodes exhibited greater catalytic activity, but elevated NO_2^- and NH_3 levels and lower N_2 concentrations were detected (89). To enhance N_2 selectivity, different routes were taken by several researchers. For instance, Zhang *et al.* electrophoretically1 deposited carbon 1nanotube onto 1Ti sheets, and then the alloys were subsequently electrodeposited utilizing different Cu/Pd atomic ratios on the Ti/CNT substrates (85). Pronkin *et al.* had a different vision in mind, electrochemical deposition of copper onto Pd particles supported by a glassy carbon cylinder (90). Nitrate electroreduction activity was enhanced by the Cu adlayer onto Pd (85).

1.6.1.5 Cu/Ni Electrode

Mattarozzi *et al*. developed a method to create porous Cu/Ni alloy (86). In fundamental solutions, microporous and sponge-like Cu/Ni alloys were used to reduce nitrate. It was explained how to electroplate porous copper onto nickel-modified graphite. The system was used in a continuous-flow configuration with a single cycle, with ammonium being the primary byproduct of the nitrate reduction process (20).

1.6.1.6 Cu/Zn Electrode

The study conducted by Yang *et al.* investigated the electroreduction of nitrate in an alkaline solution (87). The researchers utilized several Cu/Zn oxide composite electrodes, which were placed on a titanium surface using thermal decomposition (87).

1.6.1.7 Cu/MWCNT/FTO Electrode

More recently, in 2022, Nassar *et al.* modified a novel electrocatalyst used in the study of nitrate electroreduction (88). The electrocatalyst utilized in this study is a new composition consisting of nano-copper particles that are fixed onto multi-walled carbon nanotubes (MWCNTs). These nano-copper particles/MWCNTS are then spray-deposited onto substrates made of fluorine-doped tin oxide glass. Two hours of -1.80 V electrochemical reduction of nitrate resulted in a 65.40% conversion rate (88). The nanoscale size of the copper supported the high specific surface area (SSA) and catalytic activity of the modified electrode (88).

1.7 Thesis Scope

Extensive efforts and scientific investigations have been dedicated to the study of nitrate electroreduction. However, the development of electrocatalysts that possess exceptional activity, stability, and affordability for nitrate reduction while also being compatible with various aquatic environments remains a significant issue.

This study focuses on the enhancement of electrode surface area through the fabrication of nanocomposite electrodes. Composite electrodes are specifically engineered to enhance the kinetics of nitrate reduction, thereby achieving improved performance while simultaneously reducing material expenses.

In the present work, multiple routes have been taken to produce a novel electrode that achieves enhanced performance in nitrate electroreduction while simultaneously reducing costs and achieving electrode stability. To our knowledge, copper as an electrode with several modifications has been researched by several scientists, but nanoparticles offer increased catalytic surface areas, a crucial factor in enhancing the rate of electroche1mical nitrate reduction. For this purpose, copper nanoparticles wil1l be used in this research either by electrodeposition or by etching on a copper sheet.

1.8 Research Questions

1. How can highly active and stable electrocatalysts for nitrate electroreduction be developed at minimal expense?
2. How may electrode selectivity be improved such that nitrogen gas, rather than other potentially dangerous nitrate by-products, is produced?

1.9 Strategic and Technical Objectives

The issue of nitrate contamination in groundwater sources is increasingly emerging as a significant concern. Therefore, the current research study aims to resolve the issue by achieving the following strategic and technical objectives:

1. Identify a cost-effective and feasible method for the removal of nitrate from water.
2. Copper nanoparticles will be electrodeposited on a chemically pure copper sheet to increase the specific surface area (SSA).
3. A chemically pure copper sheet will be modified by chemical etching.
4. The electrodes were characterized using several techniques, including:
   - Cyclic Voltammetry (CV).
   - X-ray Photoelectron Spectroscopy (XPS).
   - Scanning Electron Microscopy (SEM).
   - Energy-Dispersive Spectroscopy (EDS).
   - X-ray Diffraction (XRD).
5. The produced electrodes will be tested for their catalytic effectiveness in the electroreduction of nitrate from purposely polluted aqueous solutions.
6. The impact of various parameters on electroreduction will be thoroughly explored (pH, temperature, nitrate concentration, electrolyte type, electrolysis potential, stability, and time).

1.10 Hypothesis

1. It is assumed that modification of the Cu electrode with copper nanoparticles should increase the SSA of the electrode and consequently increase charge transfer at the electrode/solution interface.
2. By increasing the SSA, the modification will increase selectivity towards nitrogen without residual amounts of undesirable by-products such as nitrite and ammonium ions.

1.11 Novelty

The issue of nitrate contamination in both ground and surface water is a significant global concern. This study aims to investigate practical and cost-effective methods for the elimination of nitrate ions from water. The application of electroreduction on a recently modified cathode material with high SSA is of significance in the field of de-nitration. This modification involves the electrodeposition of copper nanoparticles onto a copper sheet or the modification of the copper electrode by chemical etching. Copper nanoparticles deposited onto copper sheets or chemically etched electrodes were not mentioned or described in earlier literature as electrodes for nitrate ion electrochemical reduction in water.

The primary objective of this study is to identify a highly effective catalyst for the purpose of water purification, specifically targeting the removal of nitrate ions. The catalyst should be economically viable and provide safety while also minimizing energy consumption. The main goal is to convert nitrate into a benign substance, such as nitrogen gas (N_2). The research endeavor, which seeks to identify pragmatic approaches for removing nitrate from water sources, holds significant importance for Palestine and other nations grappling with water contamination issues.

1.2 Thesis Outline

An overview of each section is as follows:

First Chapter: Nitrate in water is briefly discussed along with its origin, health effects, basic theory, and justification for electroreduction besides an overview of emerging electrocatalysts regarding nitrate electrochemical reduction, with a primary emphasis on copper cathode. In addition, research objectives are outlined in this chapter.

Second Chapter: This chapter outlines the experimental framework and procedures employed in this thesis's research.

Third Chapter: The findings and discussion of this effort are summed up.

Fourth Chapter: Presents the thesis's final findings and recommendations for further research.

Chapter Two

Methodology

2.1 Chemicals and Reagents

All starting materials and reagents were of the highest grade available and used without further purification, they were purchased from Riedel-de Haen, Sigma Aldrich, Merck, or Frutarom. Chemicals used are Copper Sulphate, Graphene, Toluene, Sodium Sulphate, Sodium Nitrate (Source of nitrate ion), Sodium Nitrite, Anhydrous Ammonium Chloride, Ferric Chloride, Dehydrate, N-(1-Naphthyl) Ethylenediamine Dihydrochloride, Phenol (89%), Ethyl Alcohol, Sodium Hypochlorite, Sulfanilamide, Trisodium Citrate, Sodium Chloride, Sodium Hydroxide, (37%) Hydrochloric Acid, Phosphoric Acid (85%), and Sulfuric Acid (98%). Copper sheets (0.1 mm) thick have been purchased from Riedel-de Haen, (Cat # 12816).

2.2 Equipment

The spectra were measured using the Shimadzu UV-1800 Ultraviolet-visible spectrometer. The (Radwag-200/2000C/2) four-digit electrical balance accurately measured the weight of samples. The heating process was carried out using a Boekkel (107905) electric furnace. A sonicator (Power Sonic 405), pH meter (Jenway-3510), and Corrtest potentiostat (Cs350 workstation) were also employed.

XRD patterns were measured on a PAN analytical X'Pert PRO X-ray diffractometer using a Cu Kα source to characterize electrodes. XPS was measured on a Multi-Lab 2000 with a micro-focusing monochromated Al Kα X-ray (1486.6 eV) source. SEM and X-ray spectroscopy were measured with a Field-Emission SEM (FE-SEM, JEOL JSM-6700F). All SEM, EDS, XRD, and XPS characterisation were performed by the Korean Institute of Energy Research laboratories in Deajeon, South Korea.

2.3 Calibration Curve Preparations

2.3.1 Nitrate (NO_3^{-}) Calibration Curve

To prepare a stock solution of nitrate ions (NO_3^-) with a concentration of 1000 mg/L, 1.37 grams of sodium nitrate ($NaNO_3$) were dissolved in a 1000 mL volumetric flask of deionized water D.W. (91). A 100 mg/L nitrate working solution was prepared by diluting 10 mL of the stock solution in a 100 mL volumetric flask of deionized water (92).

Concentrations of 0.00, 5.00, 10.0, 20.0, 30.0, 40.0, and 50.0 mg/L were prepared by diluting the working solution with deionized water in a 100-mL volumetric flask (92). For UV-vis spectral analysis, each standard sample (92) was prepared by adding 1.0 mL of 1.00 M hydrochloric acid (HCl) to 50.0 mL of each sample.

The absorbance of each sample was measured using Simadzu UV-1800 spectra within the wavelength range of 200-400 nm. To exclude influence from dissolved organic compounds, the net absorbance of nitrate (NO_3^-) was determined by subtracting the absorbance at 220 nm from twice the absorbance at 275 nm (92). The plot of absorbance vs, concentration was constructed as a calibration curve (92).

2.3.2 NO_2^- Calibration Curve

A nitrite stock solution, with a concentration of 1000 mg/L, was created by dissolving 1.49 g of sodium nitrite ($NaNO_2$) in a 1000 mL volumetric flask of deionized water. Later, a 100 mg/L working solution was prepared by adding 10.0 mL of stock solution to a 100 mL volumetric flask of deionized water (92).

The standard samples were prepared by diluting a 100 mg/L working solution of deionized water in a volumetric flask to obtain concentrations of 1.00, 2.00, 3.00, and 4.00 mg/L.

The dye reagent solution was prepared by dissolving (1.00 g) of sulfanilamide in 80.0 mL of deionized water and 10.0 mL of phosphoric acid in a 100 mL volumetric flask. Once sulfanilamide had fully dissolved, (1.00 g) of N-(1-naphthyl)-ethylenedieamine dihydrochloride was added to the mixture and well agitated until it dissolved. At that point, deionized water was added to reach a final volume of 100 mL (92).

A volume of 1.00 mL of the dye reagent was injected to each standard sample of 25 mL. Samples were covered with a paraffin wrapper and left undisturbed for no longer than 120 minutes in order to achieve a desirable color intensity (92).

The absorbance of each sample was measured using a Shimadzu-1800 UV-vis spectrophotometer at a wavelength of 345 nm (92). The plot of absorbance vs, concentration was constructed as a calibration curve.

2.3.3 Calibration Curve for NH_4^+

An ammonium stock solution was prepared by dissolving 3.82 grams of anhydrous ammonium chloride (NH_4Cl) in a 1000 mL volumetric flask of deionized water (92). Following that, a 100 mg/L workable solution was created by diluting 10 mL of the concentrated solution in 100 mL of deionized water (92).

The standard samples were generated by diluting the working solution in a 100 mL volumetric flask of deionized water (92). The concentrations of the samples were (0, 0.25, 0.50, 0.75, 1.00, 1.50, and 2.00 mg/L).

the phenol solution was made by combining 11.1 mL of phenol (89% v/v) alongside ethyl alcohol (95% v/v) using a 100 mL volumetric flask (92).

A solution of sodiumnitroprusside (0.50% w/v) was made by dissolving 0.50 g of sodiumnitroprusside in a 100 mL volumetric flask of deionized water (92).

An alkaline citrate solution was made by dissolving 200 g of trisodium citrate and 10 g of sodium hydroxide in 1000 mL of deionized water using a 1000 mL volumetric flask. The solution was then stored in a glass container (92).

An oxidizing solution was made by combining 100 mL of alkaline citrate mixture along with 25.0 mL of sodium hypochlorite (92).

Each standard sample (25 mL) was combined with 2.50 mL of oxidizing solution, 1.0 mL of sodiumnitroprusside, and 1.00 mL of phenol solution. Subsequently, the specimens were wrapped using paraffin wrapper and placed in a sealed and lightless compartment at ambient temperature for a minimum duration of one hour (92).

The absorbance of each sample was measured using a Shimadzu-1800 UV-vis spectrophotometer at a wavelength of 640 nm (92). The plot of absorbance vs, concentration was constructed as a calibration curve.

2.4 Electrodes and Ways of Preparation

2.4.1 Bare Copper Sheet Preparation

All the copper sheets used were chemically pure. Copper sheets were cut at (1.00 cm × 5.00 cm). The sheets were pre-cleaned with sandpaper and deionized water. For further precautions sheets were dipped in sulfuric acid for no more than 20 seconds and rinsed with deionized water. Sheets were dried using nitrogen gas flow. This method was used to remove any dirt and eliminate the layer of oxidation on the substrates.

2.4.2 Bare Copper Sheet

These sheets were tested and used for comparison purposes.

2.4.3 Cu@Copper Sheet

The deposition solution used was (0.85 M $CuSO_4$. + 0.55 M H_2SO_4), and the solution was prepared using standard methods by mixing 3.18 mL H_2SO_4 with 14.25g $CuSO_4.5H_2O$ and diluted with deionized water to 500 mL (93). The solution was mixed thoroughly, covered, and set aside. A pre-cleaned copper sheet was attached to an electrochemical cell as a cathode.

Electrode Cu@Cu-1: Prepared by potentiostatic deposition at - 0.80 V for 2 minutes from (0.85 M $CuSO_4$ + 0.55 M H_2SO_4) deposition solution.

Electrode Cu@Cu-2: Prepared by potentiostatic deposition at - 0.80 V for 4 minutes from (0.85 M $CuSO_4$ + 0.55 M H_2SO_4) deposition solution.

Afterward, electrodes were rinsed with deionized water, dried using a nitrogen flow, stored in a petri dish, and then into a vacuum chamber to be used later.

2.4.4 Copper Sheets Modified by Etching

For chemical etching, two different solutions of ferric chloride were prepared (0.30 M and 0.60 M) (94).

1. Electrode Etch-Cu-1: The pre-prepared copper sheet was sunk in 0.30 M $FeCl_3$ solution for 30 seconds.
2. Electrode Etch-Cu-2: The pre-prepared copper sheet was sunk in 0.30 M $FeCl_3$ solution for 150 seconds.
3. Electrode Etch-Cu-3: The pre-prepared copper sheet was sunk in 0.60 M $FeCl_3$ solution for 30 seconds.
4. Electrode Etch-Cu-4: The pre-prepared copper sheet was sunk in 0.60 M $FeCl_3$ solution for 150 seconds.

Afterward, electrodes were rinsed with deionized water, dried using a nitrogen flow, stored in a petri dish, and then into a vacuum chamber for later use.

2.4.5 Copper Sheet Modified with Graphene

The Graphene mixture used was prepared by mixing 2.00 g of graphene with 5.00 mL of toluene. The mixture was sonicated for approximately 15 minutes in (Elmasonic S60 – Ultrasoni 7008) sonicator until it had a paint texture (95). The pre-cleaned copper sheet was painted with the graphene mixture and annealed at a temperature of 500ºC for 1 hour in a (Boekkel, 107905) furnace.

Afterward, the electrode was stored in a petri dish, and then into a vacuum chamber for later use.

2.5 Electrode Characterization

Modified electrodes have been characterized by XRD, SEM, EDS, and XPS, contrasting with earlier literature. Nanoparticle sizes were determined by the Scherer equation, while the orientation and structure of crystals were distinguished by Bragg's law.

2.5.1 X-ray Diffraction (XRD)

XRD measurements were conducted to identify the microstructure for electrodes (fresh and used Cu@Copper sheet, etched Cu sheet, and bare Cu sheet). Scherrer’s equation (2.1)(96) was used to calculate the particle sizes.

$$D = k\lambda/\beta cos\theta \quad \ldots\ldots\ldots\ldots\ldots\ldots \quad (2.1)$$

Where:

- D represents the average size of crystallites in the tested electrode.
- K is the shape factor, typically taken as value around 0.9.
- λ is the wavelength of the X-ray used for diffraction.
- β is the full width at half maximum (FWHM) of the diffraction peak.
- θ is the Bragg angle.

2.5.2 Scanning Electron Microscopy (SEM)

Surface morphologies for our prepared electrodes (fresh and used Cu@Copper sheet, etched Cu sheet, and bare Cu sheet), were examined using scanning electron microscopy.

2.5.3 Energy-Dispersive X-ray (EDS)

Elemental composition for the following electrodes, (fresh and used Cu@Copper sheet, etched Cu sheet, and bare Cu sheet) was determined with the help of an energy dispersive x-ray.

2.5.4 X-Ray Photoelectron Spectroscopy (XPS)

With the help of XPS, the chemical composition and surface oxidation states were determined for the prepared electrodes (fresh and used Cu@Copper sheet, etched Cu sheet, and bare Cu sheet).

2.5.5 Voltammetric Scanning of Nitrate Reduction

Electrochemical scanning was performed using cyclic voltammetry. Cyclic voltammetry (CV) experiments took place in a three-electrode system with the modified electrodes as the cathode electrode and the saturated calomel electrode (SCE) as the reference electrode, with the platinum plate acting as the counter electrode. Electrodes response was firstly conducted in the electrolyte solution prepared (0.05 M) Na_2SO_4 and followed up by the working solution (0.05 M Na_2SO_4 + 200 mg/L NO_3^-). All scanning experiments took place at room temperature $25 \pm 1\,°C$, all solutions were deoxygenated using nitrogen gas flow before conducting experiments. All pre-prepared

electrodes (Cu@Copper sheet, etched Cu sheet, and bare Cu sheet) were cycled from -1.80 V to -0.60 V at a 20.0 mVs^{-1} scan rate.

2.6 Electrocatalytic Reduction Experiments and Measurements

To begin the electroreduction attempts, all glassware to be operated with was precleaned with dish detergent and cleaned thoroughly with deionized water. Afterward, all stock solutions (nitrate, nitrite, and ammonium ions) and subsequent dilutions have been done using deionized water. Stock solutions were renewed weekly and stored at room temperature.

Working solutions were adjusted and prepared by the dilution of nitrate stock solution (1000 mg/L), with (0.05 M Na_2SO_4) as a supporting electrolyte solution to the anticipated concentration (200 mg/L). All working solutions were degassed by means of purging with highly purified nitrogen gas (99.999%) for approximately five minutes before the electroreduction attempt begins.

The electrocatalytic reduction experiments were conducted on aqueous nitrate solutions by Cu@Cu, Etched Cu, Graphene@Cu, and Cu electrodes (for resemblance). The electrocatalytic reduction attempts have been carried out in a 100 mL glass cell along with stirring. The electrochemical experiments were tested by a computer-controlled potentiostat (Corrtest, Cs 350) with the standard electrode configuration, all attempts were done in similar conditions. Electrode configuration is as described, platinum sheet as the counter electrode, the saturated calomel electrode (SCE) as the reference electrode, and all modified electrodes (Cu@Cu, Etched Cu, Graphene@Cu, and Cu) as the cathode (working electrode). Cathodes used in the electrochemical experiment had an active working area of 8.00 cm^2. The effective reduction of nitrate was verified by cyclic voltammetry and UV-spectrophotometry.

2.6.1 UV-spectrophotometry

The amounts of nitrate (NO_3^-), nitrite (NO_2^-), and ammonium (NH_4^+) that remain in the reaction media were measured using spectrophotometry. At specific intervals of 30 minutes, 1.50 mL samples were extracted from the reaction mixture. Each specimen is diluted with an appropriate factor and tested for the concentration of nitrate, nitrite, and ammonium ions based on the standard procedures listed above.

For nitrate ions: 0.50 mL of the specimen is taken and diluted to 10.0 mL with deionized water combined with 0.20 mL of 1.00 M HCl. The mixture undergoes spectroscopy and net absorbance was calculated by the following formula (2.2)(92).

Net Absorbance = (Abs 220 nm) – 2 (Abs 275 nm) (2.2)

The remaining 1.00 mL from the extracted specimen is diluted up to 50.0 mL with deionized water. The diluted solution is now divided into two equivalent parts 25.0 mL each (92).

For the first 25.00 mL diluted mixture, nitrite ions will be measured by adding a coloring re-agent named as naphthyl ethylenediamine and prepared by adding 80.0 mL D.W, 1.00 g sulfanilamide, and 10.0 mL (85%) phosphoric acid. The solution was sonicated to dissolve all sulfanilamide. Afterward, 1.00 g of N-(1-naphthyl) ethylenediamine dihydrochloride was added to the solution and diluted to 100 mL. 1.00 mL of the coloring solution is added to the diluted mixture. The solution is covered and saved in darkness until color develops, afterwards, absorbance is tested at 345 nm (92).

The second 25.0 mL will be tested for ammonia ions concentration, by the addition of 0.50 mL of oxidizing solution (12.5 mL (3%) sodium hypochlorite + 50.0 mL alkaline citrate solution), 1.00 mL solution of phenol (11.1 mL phenol, diluted in 100 mL 95% ethanol), and 1.00 mL of sodium nitroprusside and mixed thoroughly after the addition of each reagent. The solution is now covered by parafilm and stored in a dark cupboard at room temperature for a minimum of one hour. After the blue color is developed solutions absorbance is tested at 640 nm (92).

2.7 Different Parameters Effect on Nitrate Reduction by Electrocatalysis

2.7.1 Effect of Electrodes Type

Electroreduction of nitrate was investigated with the various electrodes prepared (Cu sheet, Two Cu@Cu electrodes (modified with different procedures), All four etched Cu sheets (Different etching methods), and Graphene@Cu). Experiments were conducted in the three-electrode electrochemical cell, experiments were done for two hours in a 100 mL cell for 80.0 mL of working solution at − 1.80 V potential, and all experiments were done at room temperature ($25 \pm 1\,^{\circ}C$). Concentration difference was tested at

different time intervals for nitrate, nitrite, and ammonium concentration in working solutions. Cu@Cu-1 plate (Electrode A as illustrated earlier) exhibited the highest electroreduction proficiency. Hence, this freshly modified electrode was chosen to complete the research.

2.7.2 Effect of Electrolyte

The effect of electrolytes was initially inspected with two different compounds (NaCl vs Na_2SO_4). One with the best effect on the electroreduction of initial nitrate concentration was chosen. Experiments were investigated with the following concentrations (0.05 M Na_2SO_4 electrolyte + 200 mg/L NO_3^- vs 0.075 NaCl + 200 mg/L NO_3^-). Experiments were done for two hours in a 100 mL cell for 80.0 mL of working solution, using Cu@Cu-1 electrode as the working electrode at − 1.80 V vs SCE, and experiments were done at room temperature. Concentration difference was tested at different time intervals by extracting 0.50 mL specimen and diluting as needed to be measured by UV-Vis spectroscopy. Na_2SO_4 (0.05 M) was preferred and chosen as an electrolyte to complete the study.

2.7.3 Effect of Applied Potential

The effect of applied potential on nitrate electroreduction was investigated. Different applied voltages were put to test (-1.50 V, -1.80 V, and 2.10 V). Experiments were done for two hours in a 100 mL cell for 80 mL of working solution, using Cu@Cu electrode as the working electrode at − 1.80 V vs SCE, and experiments were done at room temperature. Concentration difference was tested at different time intervals by extracting 0.50 mL specimen and diluting as needed to be measured by UV-Vis spectroscopy.

2.7.4 Effect of Primary NO_3^- Concentration

Different initial nitrate concentrations were researched by the electroreduction procedure. The study was done at four different initial concentrations (200 mg/L, 400 mg/L, 600 mg/L, and 800 mg/L) in addition to a 0.05 M Na_2SO_4 electrolyte. Experiments were done for two hours in a 100 mL cell for 80.0 mL of working solution, using Cu@Cu-1 electrode as the working electrode at −1.80 V vs SCE, and experiments

were done at room temperature. Concentration difference was tested at different time intervals by extracting 0.50 mL aliquots of working solution and diluting as needed to be measured by UV-Vis spectroscopy.

2.7.5 Effect of Temperature

The effect of different temperatures on the electroreduction of nitrate was researched. By carrying the electroreduction of nitrate experiments at three different temperatures ($10\ °C$, $25\ °C$, and $35\ °C$). Experiments were done for two hours in a 100 mL cell for 80.0 mL of working solution, using Cu@Cu-1 electrode as the working electrode at -1.80 V vs SCE. Concentration difference was tested at different time intervals by extracting 0.50 mL specimen and diluting as needed to be measured by UV-Vis spectroscopy.

2.7.6 Effect of Time

Electroreduction of nitrate working solution was examined over a long period of time (Seven Hours). Experiments were conducted in the three-electrode electrochemical cell, experiments were done for two hours in a 100 mL cell for 80.0 mL of working solution at -1.80 V vs SCE, and all experiments were done at room temperature ($25 \pm 1\ °C$). Concentration differences were tested at different time intervals for nitrate, nitrite, and ammonium, by extracting 1.50 mL aliquots from the working solution. Dilution to the appropriate percentage was done and samples were measured by UV-Vis spectroscopy.

2.7.7 Electrode Stability

To test the performance and stability of the newly proposed Cu@Cu-1 electrode, one freshly prepared electrode was used repeatedly in three experiments with similar parameters. Experiments were conducted in the three-electrode electrochemical cell. Experiments were done for two hours in a 100 mL cell for 80.0 mL of working solution at -1.80 V vs SCE at room temperature ($25 \pm 1\ °C$). Concentration difference was tested at different time intervals by extracting 0.50 mL specimen and diluting as needed to be measured by UV-Vis spectroscopy.

Chapter Three

Results and Discussions

3.1 Cu@Cu Sheet Electrode

Cu@Cu-1 and Cu@Cu-2 electrodes were modified by potentiostatic Cu deposition from (0.85 M $CuSO_4$ + 0.55 M H_2SO_4) at - 0.80 V at different time intervals. Cu@Cu-2 was eliminated from the nitrate electroreduction study due to inadequate adherence between Cu nanoparticles and copper sheets.

3.1.1 Interpretations

3.1.1.1 SEM Inspection

SEM images of the electrode top-view and cross-sectional area are illustrated below in Figure 3.1 (a), (a'), (b), and (b') of fresh Cu@Cu-1 and used Cu@Cu-1 respectively. The images represent the Cu@Cu-1 electrode in both forms fresh and used in an electrocatalytic reduction experiment. Both electrodes were obtained by Cu deposition under the same conditions by using similar solutions.

Figure 3.1

SEM micrographs of (a) Fresh Cu@Cu-1 and (b) Used Cu@Cu-1

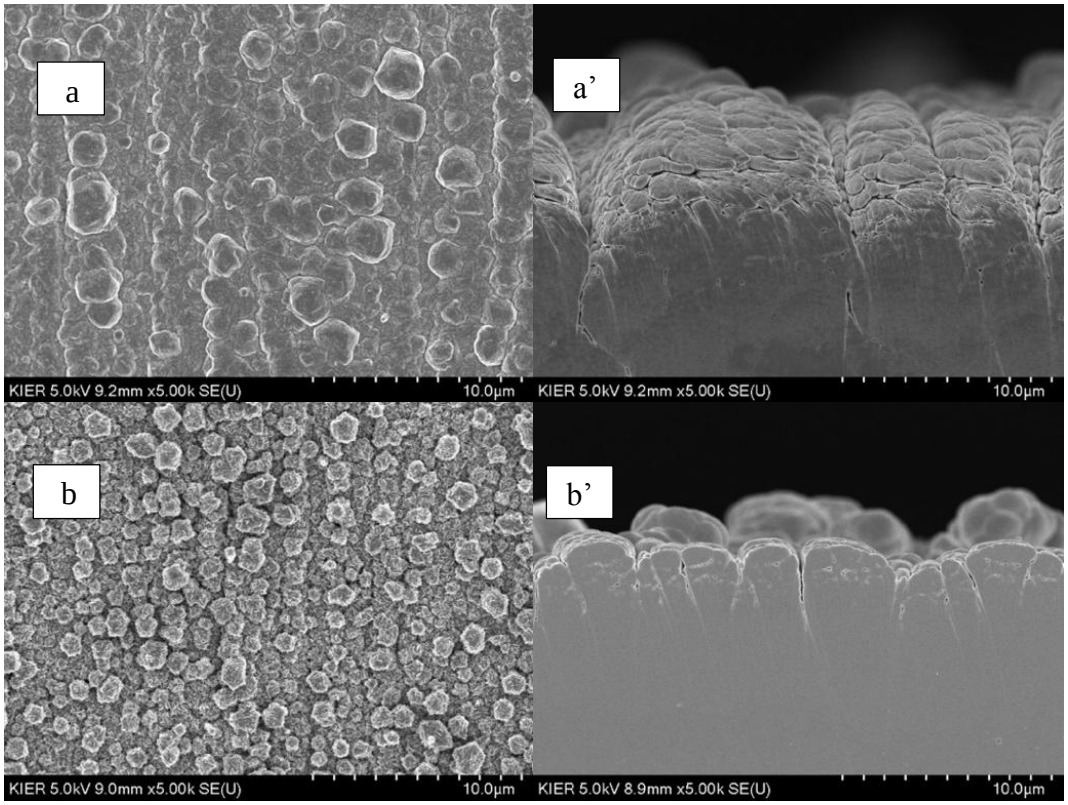

The provided images (a) and (a') exhibit compelling empirical support for the growth of compact copper nanoparticles of diverse dimensions on the surface of the copper sheet. The analysis reveals that the average particle size was 168.1 nm, and the film exhibited a thickness of around 2.98 μm.

On the other hand, images (b) and (b') in Figure 3.1 represent a Cu@Cu-1 electrode used in nitrate electroreduction. The particle size obtained for the used electrode had an average size of 112.6 nm, and the Cu film exhibited a thickness of approximately 3 μm. After undergoing electrocatalysis, copper crystallites exhibited a distinct transformation, acquiring sharp edges resembling flakes. These crystallites were found to be randomly dispersed across the electrode. Furthermore, SEM analysis reveals that the particle size and thickness indicate a distinct transformation from large copper agglomerates to smaller agglomerates and crystallites. Following electrocatalysis, the nanoparticles have acquired well-defined edges, resulting in the formation of agglomerates with a distinctive flower-like morphology.

3.1.1.2 Cu@Cu XRD Investigation

Cu@Cu-1 electrode crystal structures of new and used electrodes were investigated by X-ray diffraction analysis (XRD, as shown in Figure A.1. In the XRD display for Cu@Cu-1 electrode, signals obtained are at 2θ = 43.38 (111), 50.52 (200), and 74.20 (220) these signals are accredited to Cu (JCPDS, 65-9743) (97,98).

Signals observed for used Cu@Cu-1 are at 43.42 (111), 50.54 (200), and 74.20 (220), signals obtained are associated with Cu (JCPDS, 65-9743) (97,98). It was noticed that the peak was sharper on the used electrode, indicating an increase of crystallinity of nanoparticles, similar to the indications noticed in the SEM images presented in Figure 3.1. However, both electrodes achieved similar indications with unnoticeable differences. Particle sizes of deposited Cu were investigated using an XRD pattern and Scherer equation, the average particle size was found to be 54.57 nm.

Table 3. 1

Breakdown of XRD patterns of Cu@Cu-1 and used Cu@Cu-1

Electrode	$2\theta°$	d ((Å)	Species	Particle size (nm)	FWHM	(hkl)
Cu@Cu-1	43.38	2.0860	Cu	74.45	0.1200	(111)
	50.52	1.8066	Cu	45.89	0.2000	(200)
	74.20	1.2781	Cu	43.37	0.2400	(220)
Used Cu@Cu-1	43.42	2.0841	Cu	55.84	0.1600	(111)
	50.54	1.8060	Cu	45.54	0.2000	(200)
	74.20	1.2781	Cu	52.05	0.2000	(220)

Overall, Table 3.1 reviews XRD patterns, particle sizes, and species of Cu@Cu-1 and used Cu@Cu-1 electrodes. The patterns reveal that the deposited particles on the copper sheet are all Cu therefore, Cu@Cu-1 was chosen to complete the study. The used electrode XRD results are very promising and indicate the stability of the electrode.

Due to technical complications and transportation restraints, XRD analysis was performed after 5 weeks of preparation.

A comparison between the SEM morphologies and the XRD results obtained It was noticed that particle sizes obtained by SEM are larger compared with particle sizes obtained by the Scherer equation using XRD, as illustrated in Table 3.1. This suggests that the particles derived from the various characterization approaches exhibit dissimilarities. The X-ray diffraction (XRD) pattern depicted in Figure A.1 yields insights into the average dimensions of the crystalline particles. Conversely, the scanning electron microscopy (SEM) pictures in Figure 3.1 display larger agglomerates. As a result, each SEM-detected agglomeration is made up of numerous smaller crystallites, as evidenced by XRD patterns.

3.1.1.3 Cu@Cu EDS Examination

The elemental analysis of Cu@Cu-1 conserved and consumed electrodes are exhibited in Table 3.2. It's clearly established that the unused electrode contains 83.53 weight % of Cu while the used electrode comprises 83.16 weight % of Cu.

The copper content in electrodes has only decreased slightly, while the oxygen content has barely increased when used in the electroreduction of nitrate. This indicates the effective stability of the Cu@Cu-1 tailored electrode.

Table 3.2

Comparison between Cu@Cu-1 and electrodes reported in the literature

Fresh Cu@Cu-1			Used Cu@Cu-1		
Element	Wt%	Atomic %	Element	Wt%	Atomic %
C	12.72	40.60	C	11.93	38.53
O	3.75	9.00	O	4.91	11.29
Cu	83.53	50.41	Cu	83.16	50.18
Total:	100.00	100.00	Total:	100.00	100.00

3.1.1.4 XPS Analysis of Cu@Cu

XPS was performed for an advanced investigation of the deposited coat components. The XPS spectra of Cu@Cu-1 electrode is represented in Figure 3.2, involving high-resolution spectra of Cu 2p and O 1s peaks. In Figure A.2, XPS spectra of used Cu@Cu-1 are reported, including high-resolution Cu 2p and O 1s.

For the Cu@Cu-1 electrode, XPS spectra gave a peak for Cu 2p at 932.13 eV; in fresh Cu@Cu-1, the Cu 2p peak was detected at 932.02. The binding energy of Cu 2p corresponds to Cu $2p^{3/2}$ and it implies the possible availability of Cu (II), Cu (I), and Cu (0) (99). For both electrodes, Cu@Cu-1 and Used Cu@Cu-1, the O 1s peak was indicated to be at 531.13 eV. This peak may have been a result of the presence of O 1s in other constituents where oxygen is present, similar to carbonates (100). The C 1s peak spotted in the spectra is a result of hydrocarbon from the XPS instrument.

Figure 3.2

XPS spectra of Cu@Cu-1, (a) Complete spectra, (b) Cu 2p peak, and (c) O 1s peak

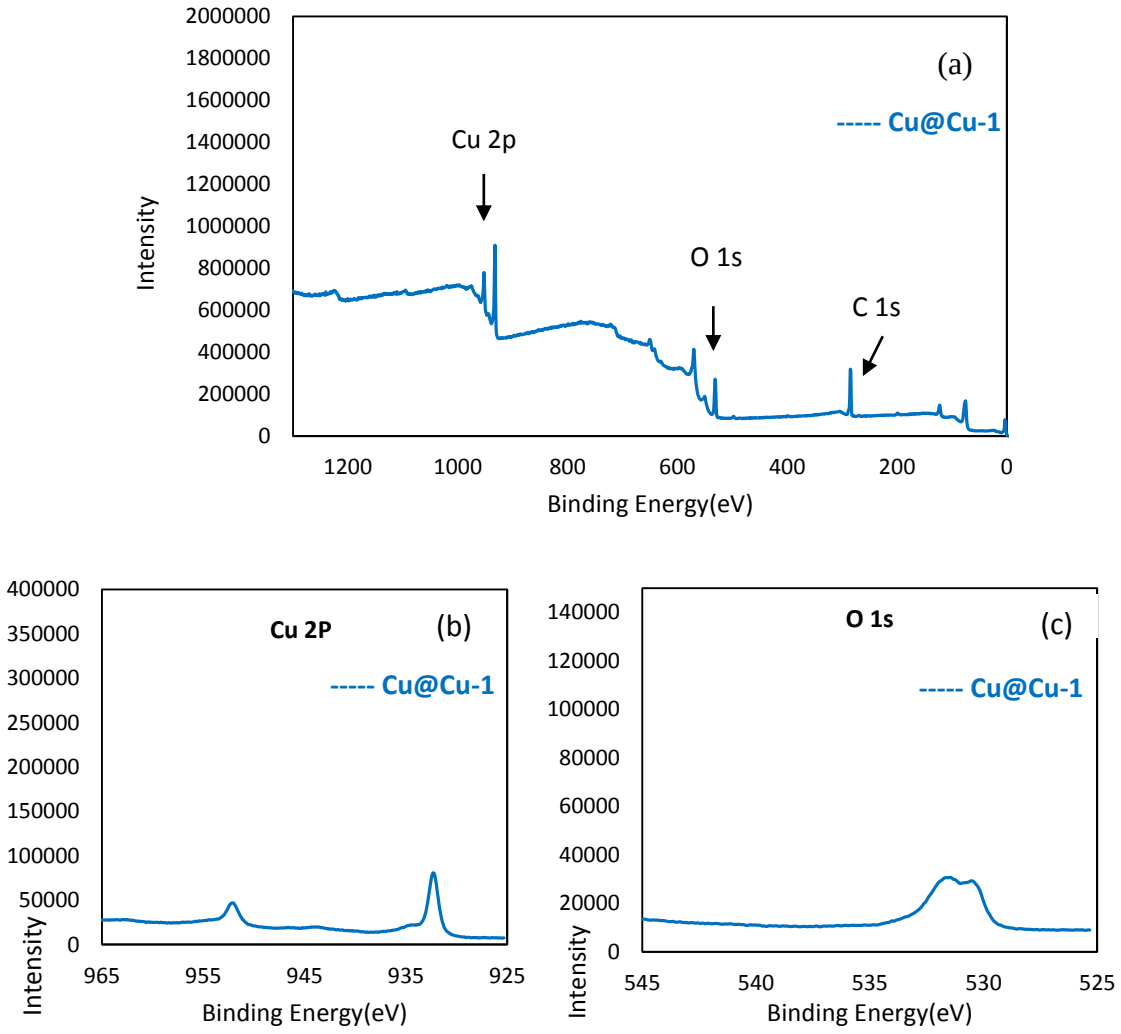

3.1.1.5 Cyclic Voltammetry Examination

In Figure A.3 a cyclic voltammogram is represented for Cu sheet in (0.05 M Na_2SO_4) blank in comparison with the working solution (0.05 M Na_2SO_4 + 200 mg/L NO_3^{-}).

The cyclic voltammogram obtained for Cu@Cu-1 in (0.05 M Na_2SO_4) blank in comparison with the working solution (0.05 M Na_2SO_4 + 200 mg/L NO_3^{-}) is represented in Figure 3.3. The modified electrodes cyclic voltammogram indicates a clear increase in the overall reduction current with different scan voltages with the existence of nitrate in contrast with the 0.05 M Na_2SO_4 blank solution. This verifies the electrode's capability for nitrate reduction.

Figure 3.3

Cyclic voltammogram on Cu@Cu-1 in ~~0.05~~ M Na_2SO_4 and in (0.05 ~~M~~ Na_2SO_4 + 200 mg/L NO_3^{-})

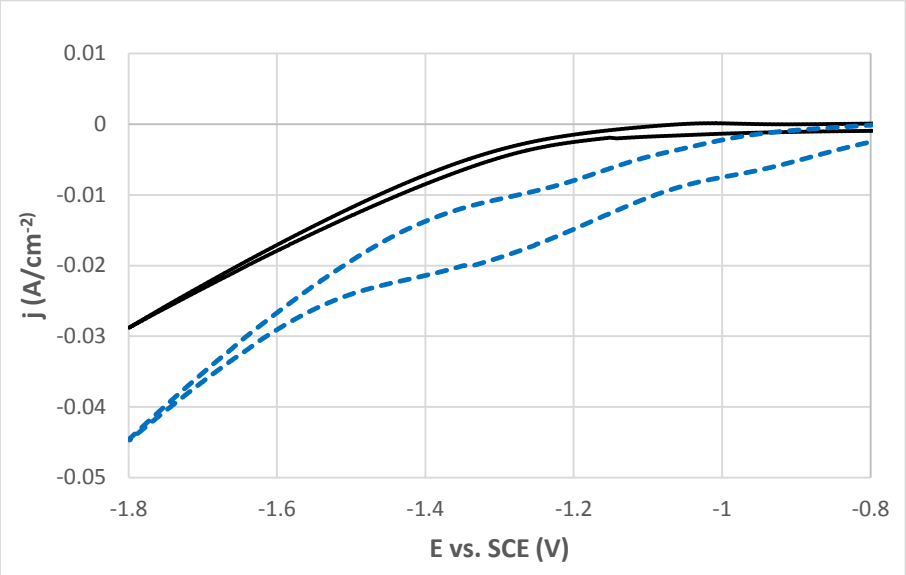

3.1.2 Nitrate Electroreduction

Cu@Cu-1 electrode modified by potentiostatic Cu deposition at - 0.80 V from (0.85 M $CuSO_4$ + 0.55 M H_2SO_4) for 2 minutes was chosen and used to experiment nitrate electroreduction since Cu@Cu-2 prepared with similar conditions but with a different time interval (4 minutes) was eliminated due to the poor adherence between the copper sheet and copper nanoparticles.

3.1.2.1 Nitrate Electroreduction Experiments

The electroreduction of nitrate trial was run for 120 minutes of electrolysis at -1.80 V using Cu, and Cu@Cu-1 as working electrodes. The Cu sheet was used for evaluation purposes.

3.1.2.2 Influence of Type of Electrode

The influence of electrode type was determined based on nitrate conversion percent.

Conversion percent was estimated based on equation 3.1.

$$Nitrate\ (NO_3^-)\ Conversion\ Percentage = \frac{C_i - C_t}{C_i} \times 100\%. \quad \text{.....(3.1)}$$

Where C_i stands for the initial concentration of NO_3^- and C_t is the nitrate concentration at any known time. Nitrate conversion percentages, by potenstiostatic electroreduction at -0.80 V for 120 minutes by Cu and Cu@Cu-1 working electrodes are demonstrated in Figure 3.4.

Figure 3.4

Nitrate conversion percentage on Cu, and Cu@Cu-1 vs electrolysis time. Experiments were conducted using (80 mL; 0.05 M Na_2SO_4 + 200 mg/L NO_3^-), 120 min, 25 ± 1℃, and -1.80 V vs. SCE

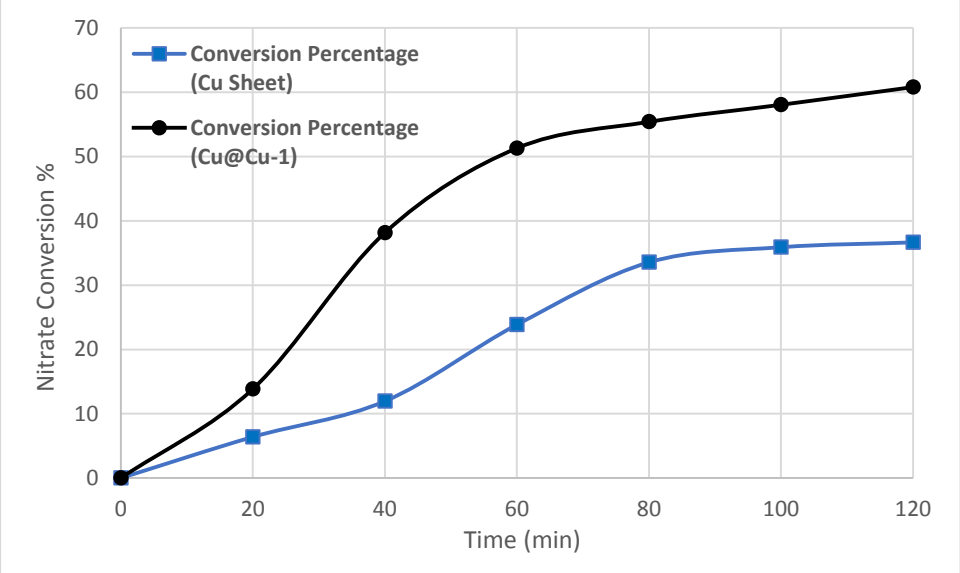

Cu sheet and Cu@Cu-1 resulted in 36.65% and 60.8%, respectively, under similar circumstances. Cu@Cu-2 wasn't used in those trials due to the poor adherence between the sheet and nanoparticles, as mentioned previously.

Nitrate, nitrite, and ammonium ions variations in working solutions for Cu, and Cu@Cu-1 are illustrated below in Figure 3.5 (a) and (b), respectively, for 120 minutes of electrolysis. There is a variation between the results presented in Figure 3.5 for both electrodes, it clearly appears that the Cu@Cu-1 electrode has better nitrate electroreduction than the Cu sheet electrode. Figure 3.5 also revealed that ammonium is the major byproduct for the Cu sheet during the 120 minutes of electrolysis.

Figure 3.5

Nitrate, nitrite, and ammonium concentrations vs. electrolysis time

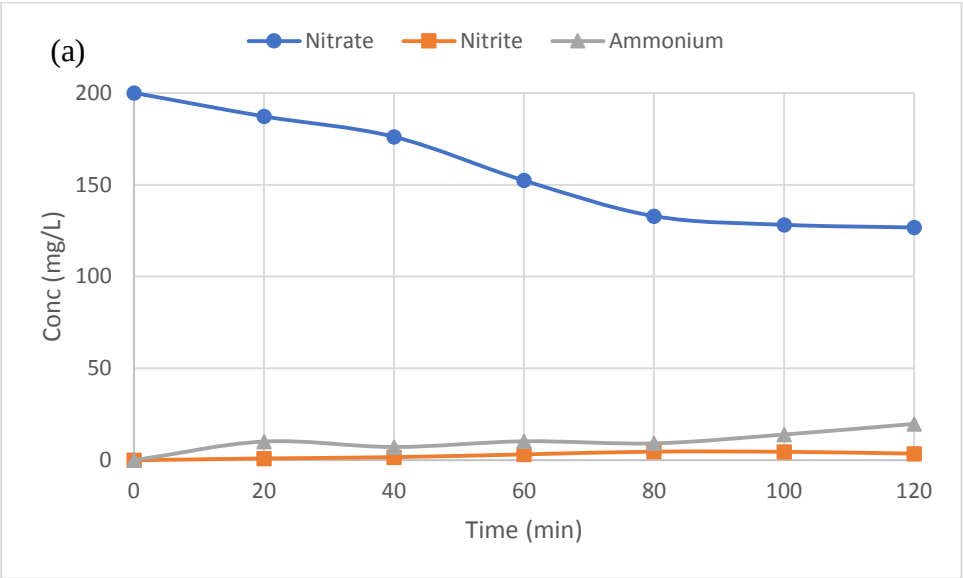

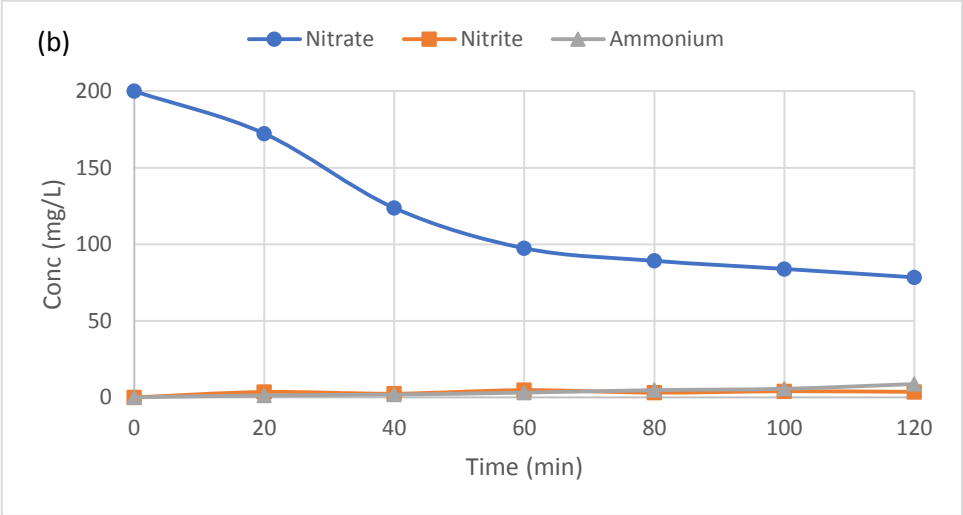

by (a) Cu sheet, and (b) Cu@Cu-1 modified electrode. All experiments were conducted by means of (80 mL; 0.05 M Na_2SO_4 + 200 mg/L NO_3^-), 120 min, 25 ± 1℃, and -1.80 V vs. SCE

Selectivity percentage (S%) for byproducts; nitrite (S NO_2^- %), ammonium (S NH_4^+ %), and dinitrogen gas (S N_2 %) were calculated by means of equations (3.2), (3.3), and (3.4) respectively, presuming that other quantities of byproducts resulting from nitrate electroreduction, for instance, nitrous oxide, hydrazine, or hydroxylamine are insignificant (101–103). Selectivity values (S%) were estimated as fractions of yielded moles per product to the reduced moles of NO_3^- multiplied by a hundred (49,104,105).

$$S\ NO_2^-\ (\%) = \frac{[NO_2^-]_t}{[NO_3^-]_{initial} - [NO_3^-]_{final}} \times 100 \quad \text{.... (3.2)}$$

$$S\ NH_4^+\ (\%) = \frac{[NH_4^+]_t}{[NO_3^-]_{initial} - [NO_3^-]_{final}} \times 100 \quad \text{.....(3.3)}$$

$$S\ N_2\ (\%) = 100\% - [S\ NO_2^-\ \% + S\ NH_4^+\ \%] \quad \text{.....(3.4)}$$

In the above equations $[NO_3^-]$, $[NO_2^-]$, and $[NH_4^+]$ all signify the molar concentration of ions in the working solution. Selectivity values for byproducts that resulted from nitrate electroreduction by electrolysis and employing Cu sheet and Cu@Cu-1 as working electrodes (cathode) are all listed in Table 3.3.

Table 3.3

*Selectivity for byproducts (nitrite, ammonium, or dinitrogen gas) on Cu or Cu@Cu-1. All experiments were conducted by means of (80 mL; 0.05 M Na_2SO_4 + 200 mg/L NO_3^-), 120 min, 25±**1**℃, and -1.80 V vs. SCE*

Electrode	$[NO_3^-]$ *Conversion* % (*Based on mg L^- Conc.*)	S% (*Based on molar Conc.*)		
		NO_2^-	NH_4^+	N_2
Cu sheet	36.65	6.64	92.82	0.54
Cu@Cu-1	60.80	3.99	24.59	71.42

The result of the electrochemical reduction done for nitrate by Cu@Cu-1 has been promising compared to the reduction process done by Cu sheet under similar conditions. The nitrate conversion percentage by Cu sheet has been reported to be 36.65%, while for Cu@Cu-1 the reported result is 60.8 % and it has exceeded Cu sheet results.

The difference between the conversion percentage for both electrodes is approximately 24.15% giving Cu@Cu-1 a greater advantage than the Cu sheet. Although the difference is quite high, it's not the only characteristic for Cu@Cu-1, the selectivity rate towards nitrogen due to the electrocatalysis done by Cu@Cu-1 is found to be 71.42% while on the other hand, Cu sheet only reported only 0.54% nitrogen selection since Cu sheet has a higher selectivity percentage towards NH_4^+, in this research and based on previous literature (69).

3.2 Etched Copper Sheets

Electrodes Etch-Cu-1, Etch-Cu-2, Etch-Cu-3, and Etch-Cu-4 were modified by the etching method using $FeCl_3$ as an etching solution. Electrodes Etch-Cu-1 and Etch-Cu-2 were etched by 0.3 M $FeCl_3$ at different time intervals 30 seconds and 150 seconds, respectively. Electrodes Etch-Cu-3 and Etch-Cu-4 were altered by a 0.6 M $FeCl_3$ etching solution at different time intervals 30 seconds and 150 seconds respectively.

Nitrate reduction was tested for all four electrodes, although electrodes Etch-Cu-3 and Etch-Cu-4 were very weak after being altered by the etchant solution and didn't pass the test of strength, they were broken down into pieces directly after the process of reduction.

Electrodes Etch-Cu-2 and Etch-Cu-4 represented higher strength; nevertheless, nitrate reduction results weren't very promising. Electrode Etch-Cu-2 was selected to complete the research because it exhibited higher reduction rates than the other etched electrodes.

3.2.1 Characterization

3.2.1.1 SEM Analysis

Surface and cross-section SEM image representations of the Cu-etched (Electrode Etch-Cu-2) are shown in Figure 3.6 (a) and (a') respectively.

Figure 3.6

SEM micrographs of (a) Surface Etch-Cu-2 and (b) Cross section Etch-Cu-2

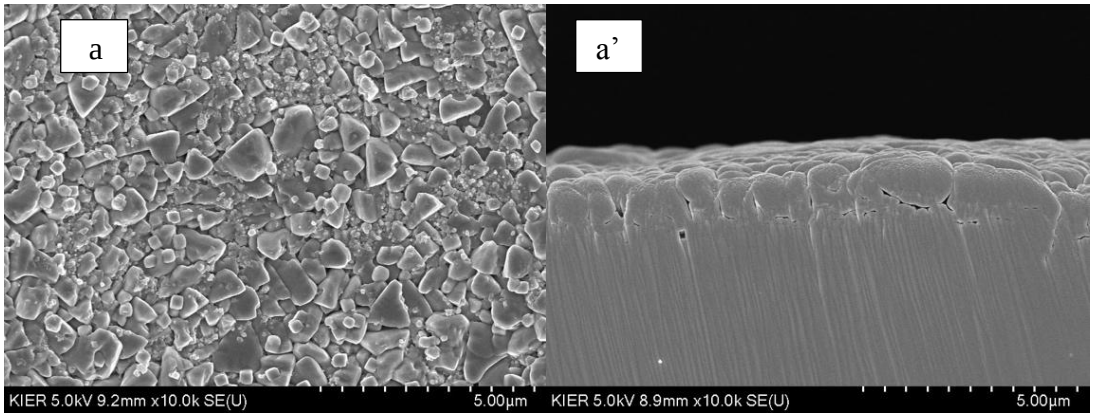

Following the etching procedure, a noticeable transformation in the electrode's appearance has taken place. The once uniform surface of a typical copper sheet now exhibits noticeable roughness, as depicted in Figure 3.6 (a). The electrode surface has

irregularities and regions with varying textures and morphologies. Nevertheless, this irregularity is not uniformly distributed across the electrode surface; rather, it manifests as a non-uniform topography characterized by variations in size and shape. The electrode surface has irregularities and regions with varying textures and morphologies.

3.2.1.2 Etched Cu-2 EDS Examination

The elemental analysis of Etched Cu -C is exhibited in Table 3.4. It's clearly established that the etched Cu-2 electrode contains 74.66 weight % of Cu, along with 5.30 weight % O, 13.77% C, and 6.27 weight % Cl. The Cl content in this electrode is an impurity caused by the etchant solution.

Table 3.4

Elemental analysis by EDS of Etched Cu-2

Element	Wt%	Atomic %
C	13.77	40.52
O	5.30	11.70
Cl	6.27	6.25
Cu	74.66	41.53
Total:	100.00	100.00

3.2.1.3 Etched Cu-2 XRD Investigation

X-ray diffraction (XRD) analysis was used to investigate the crystal structures of an etched Cu-2 electrode, Figure A.4. The XRD signals for etched Cu-2 electrode were obtained at 2θ = 43.40 (111), 50.52 (200), and 74.18 (220). These signals are accredited to Cu (JCPDS, 65-9743) (97,98). As well to a signal obtained at 2θ = 28.58 (110) this signal is related to Cu_2O (JCPDS, 05-0667)(106,107). Particle sizes of etched Cu were investigated using information given by XRD and Scherer equation.

Table 3.5

Breakdown of XRD pattern of Etched Cu-2 electrode

Electrode	$2\theta°$	d (Å)	Species	Particle size (nm)	FWHM	(hkl)
Etched Cu-2	28.58	3.1234	Cu_2O	71.38	0.1200	(110)
	43.40	2.0850	Cu	74.45	0.1200	(111)
	50.52	1.8066	Cu	57.37	0.1600	(220)
	74.18	1.2784	Cu	52.04	0.2000	(200)

Overall, Table 3.5 reviews XRD pattern, particle sizes, and species of etched Cu-2 electrode. The pattern reveals that the copper sheet contains Cu particles along with Cu_2O. The presence of Cu_2O particles indicates oxidation of the electrode.

Due to technical complications and transportation restraints, XRD analysis was performed after 5 weeks of preparation.

3.2.1.4 XPS Analysis of Etched Cu-2

XPS was performed for an advanced investigation of the etched layer components. XPS spectra of the Cu-2 electrode are represented in Figure A.5, involving high-resolution spectra of Cu 2p and O 1s peaks.

The XPS analysis of the Cu-2 electrode revealed a peak for Cu 2p at 932.05 eV. The binding energy of Cu 2p corresponds to Cu $2p^{3/2}$ and is indicative of the potential presence of Cu (II), Cu (I), and Cu (0) species (99). The O 1s peak was indicated to be at 531.55 eV. This peak may have been a result of the presence of O 1s in other constituents where oxygen is present, similar to carbonates (100), or it could indicate the oxidation of the copper sheet since Cu_2O particles are present in the XRD pattern as shown in Table 3.5. The presence of the C 1s peak observed in the spectra can be attributed to the hydrocarbon contamination originating from the XPS equipment.

3.2.1.5 Etched Cu-2 Cyclic Voltammetry Examination

The cyclic voltammogram for Etched Cu-2 in a blank solution of 0.05 M Na_2SO_4, compared to the working solution of 0.05 M Na_2SO_4 with 200 mg/L NO_3^-, is depicted in Figure A.6. The cyclic voltammogram of the modified electrodes shows a minor rise in the total reduction current when different scan voltages are applied in the presence of nitrate, as compared to the blank solution containing 0.05 M Na_2SO_4. This validates the electrode's capacity for nitrate reduction.

3.2.1.6 Nitrate Electroreduction

Etched copper electrodes modified by chemical etching were used to experiment with nitrate electroreduction.

3.2.1.7 Nitrate Electroreduction Experiments

The electroreduction of nitrate trial was run for 120 minutes of electrolysis at -1.80 V using all four etched copper sheets as working electrodes. The Cu sheet was used for evaluation purposes.

3.2.1.8 Influence of Type of Electrode

The influence of electrode type was determined based on nitrate conversion percent. Conversion percent was estimated based on equation 3.1.

Nitrate conversion percentages by potenstiostatic electroreduction at -1.80 V for 120 minutes by Etch-Cu-1, Etch-Cu-2, Etch-Cu-3, Etch-Cu-4, and Cu sheet working electrodes are demonstrated in Figure 3.7. Etch-Cu-1, Etch-Cu-2, Etch-Cu-3, Etch-Cu-4, and Cu resulted in 32.6%, 45.7%, 28.8%, 28.3%, and 36.65%, respectively under similar circumstances.

Only the Etch-Cu-2 electrode from the working electrodes modified by chemical etching exhibited a higher nitrate reduction than the Cu-sheet.

Figure 3.7

Nitrate conversion percentage on etched electrodes and Cu sheet vs. electrolysis time. Experiments were conducted using (80 mL; 0.05 M Na_2SO_4 + 200 mg/L NO_3^{-}), 120 min, 25 ± 1℃, and -1.80 V vs. SCE

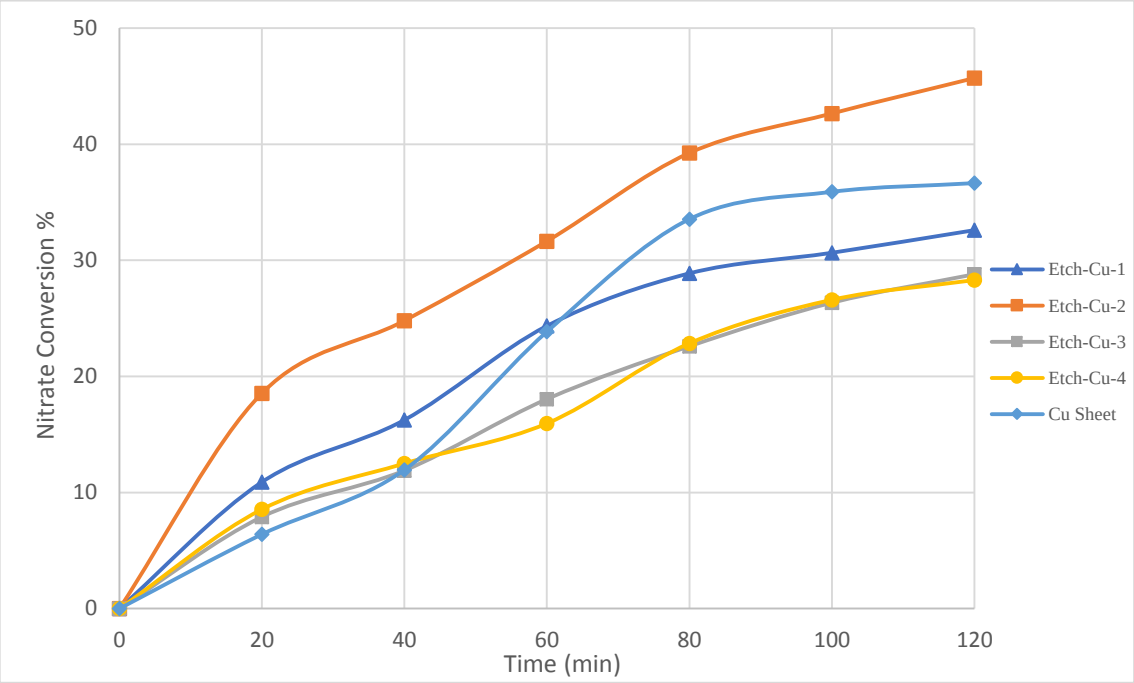

There is a variation between the results presented in Figure 3.7 when compared to the Cu-sheet presented above in Figure 3.5 (a), it clearly shows that the modified Etch-Cu-2 electrode achieved higher nitrate reduction rates than Cu-sheet electrode. Nitrate, nitrite, and ammonium ions variations in working solutions for Etch-Cu-2 are illustrated in Figure A.7 for 120 minutes of electrolysis. Figure A.7 also revealed that Etch-Cu-2 had higher ammonium concentration as by-product of nitrate reduction during the 120 minutes of electrolysis.

Table 3.6

Selectivity for byproducts (nitrite, ammonium, or dinitrogen gas) on Etch-Cu-2. All experiments were conducted by means of (80 mL; 0.05 M Na_2SO_4 + 200 mg/L NO_3^{-}), 120 min, 25±1℃, and -1.80 V vs. SCE

Electrode	$[NO_3^-]$ *Conversion* % (Based on mg L^- Conc.)	S%(Based on molar Conc.)		
		NO_2^-	NH_4^+	N_2
Etch-Cu-2	45.7	3.04	71.07	25.89

Selectivity percentage (S%) for byproducts; nitrite (S NO_2^- %), ammonium (S NH_4^+ %), and dinitrogen gas (S N_2 %) were calculated by means of equations (3.2), (3.3), and (3.4) respectively.

The electrochemical reduction of nitrate using Etch-Cu-2 resulted in a yield of 45.7%, which is higher than the stated yield of 36.65% achieved using a Cu sheet. This indicates that Etch-Cu-2 offers a significant advantage in terms of efficiency. However, the conversion of nitrate to non-hazardous nitrogen gas in Etch-Cu-2 was found to be just 25.89%, indicating that the desired level of selectivity was not achieved. The properties of Cu were only slightly improved with chemical etching, as evidenced by a larger selectivity percentage towards NH_4^+. This finding aligns with earlier literature (69).

3.3 Graphene/Copper Sheet

The investigation of copper sheet modification using graphene was conducted in order to improve the electroreduction of nitrate. Graphene was made ready through the incorporation of 2 g of graphene and 5 mL of toluene (95). This mixture underwent sonication and stirring until it achieved a consistency mimicking that of paint. The copper sheet, which had undergone pre-cleaning, was coated with the graphene mixture and subjected to annealing at a temperature of 500°C for a duration of 1 hour.

However, after alterations were done, it was revealed that the copper sheet exhibited increased brittleness, and the adhesion between the graphene and copper sheet proved to be notably feeble, resulting in detachment upon the initiation of electrolysis.

The outcomes obtained from the investigation on nitrate electroreduction employing the copper sheet modified by graphene were unsatisfactory. Therefore, graphene-modified copper sheets were omitted and the research regarding graphene was stopped short.

Since the newly modified Cu@Cu-1 electrode exhibited the highest nitrate conversion efficiency compared to other electrodes investigated in this study, all subsequent sections of the investigation will be restricted to the Cu@Cu-1 electrode.

3.4 Factors Effecting Cu@Cu-1 Efficiency

3.4.1 Effect of Applied Voltage

The data presented in Figure A.8 illustrates the varying levels of nitrate conversion seen under various applied potentials. According to the data presented in the figure, the nitrate conversion percentage values were observed to be 56.4%, 60.8%, and 64.1% within a time frame of 120 minutes, corresponding to applied potentials of -1.50 V, -1.80 V, and -2.10 V vs. SCE, respectively.

The observed rise in the percentage of nitrate conversion exhibits only a marginal increase upon raising the applied voltage. This phenomenon can be attributed to the increased electromotive force for electrons at the cathode when subjected to greater voltage levels. The catalytic efficiency of the electrode is greatly influenced by its composition and the relative position of the charge distribution on its surface.

For all subsequent studies, a consistently applied potential of -1.80 V was utilized. This decision was made due to the observed minimal difference in the efficiency of nitrate electroreduction while applying a potential of -2.10 V. Additionally, selecting a voltage of -1.80 V would be more advantageous option from an economic standpoint. As a matter of fact, the voltage utilized in certain scholarly works has a significantly greater magnitude when compared to the aforementioned values (79,108).

3.4.2 Effect of Electrolyte Type

The data presented in Figure 3.8 illustrates the relationship between the percentage of nitrate conversion and the elapsed time when utilizing 0.05 M Na_2SO_4 and 0.075 M NaCl as the electrolyte. The observed percentage of nitrate conversion was found to be slightly higher when a 0.05 M Na_2SO_4 solution was employed, compared to the percentage obtained when a 0.075 M NaCl solution was utilized. Specifically, the recorded values for nitrate conversion were 60.8% and 54.7% respectively.

Figure 3.8

Nitrate conversion percentage vs electrolysis time with different electrolytes. Experiments were conducted using (80 mL; 0.05 M Na_2SO_4 + 200 mg/L NO_3^{-}), and (80 mL; 0.075 M NaCl + 200 mg/L NO_3^{-}). For 120 min, 25 ± 1℃, and -1.80 V vs. SCE

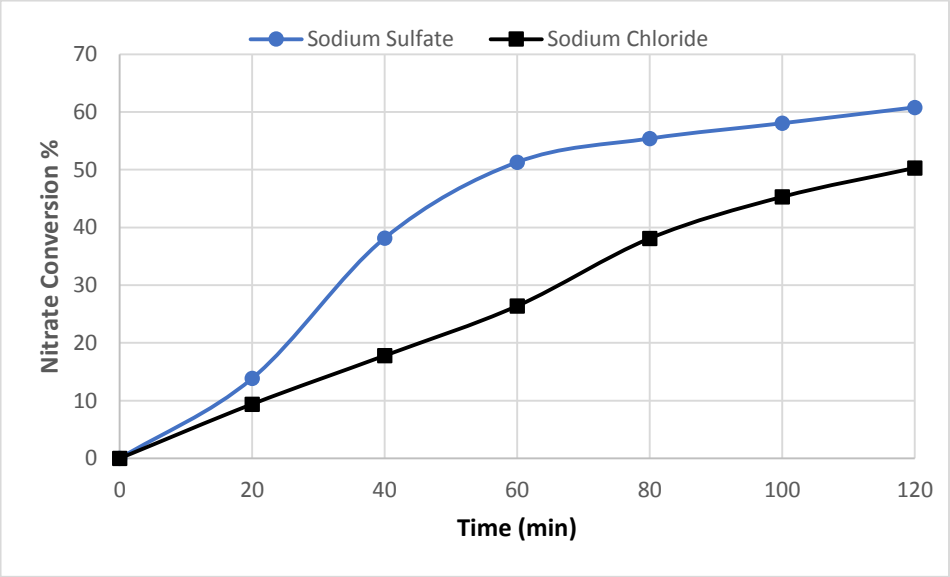

3.4.3 Effect of Temperature

Cu@Cu-1 electrode ability to electro-reduce nitrate has been studied in the (15–35℃) temperature range. The findings are represented in Figure A.9. The results indicate that the nitrate conversion percentages at temperatures of 15 ℃ and 35 ℃ were 56.9% and 66.02% correspondingly. The observed enhancement in the nitrate conversion efficiency upon increasing the temperature can be attributed to the accelerated diffusion rate of nitrate ions toward the electrode surface from the solution's bulk (109).

Nevertheless, the findings indicate that temperature does not have a statistically significant impact on the process of electroreduction. The investigation of the impact of temperature on electroreduction has been limited in earlier studies. This study focused on a narrow temperature range due to the limited impact of temperature on the nitrate electroreduction process. The temperature utilized in this study was consistently maintained at 25 ± 1 ℃, as indicated in the Experimental Sections, unless explicitly specified differently.

3.4.4 Effect of Prolonged Time

The figure labeled as Figure 3.9 displays the changes in the concentrations of nitrate, nitrite, and ammonium over a period of 420 min during the process of electrolysis using the newly proposed Cu@Cu-1 electrode at a potential of -1.80 V vs SCE.

Figure 3.9

Nitrate, nitrite, and ammonium concentrations vs. electrolysis time by Cu@Cu-1 modified electrode. All experiments were conducted by means of (80 mL; 0.05 M Na_2SO_4 + 200 mg/L NO_3^{-}), 420 min, 25 ± 1℃, and -1.8 V vs. SCE

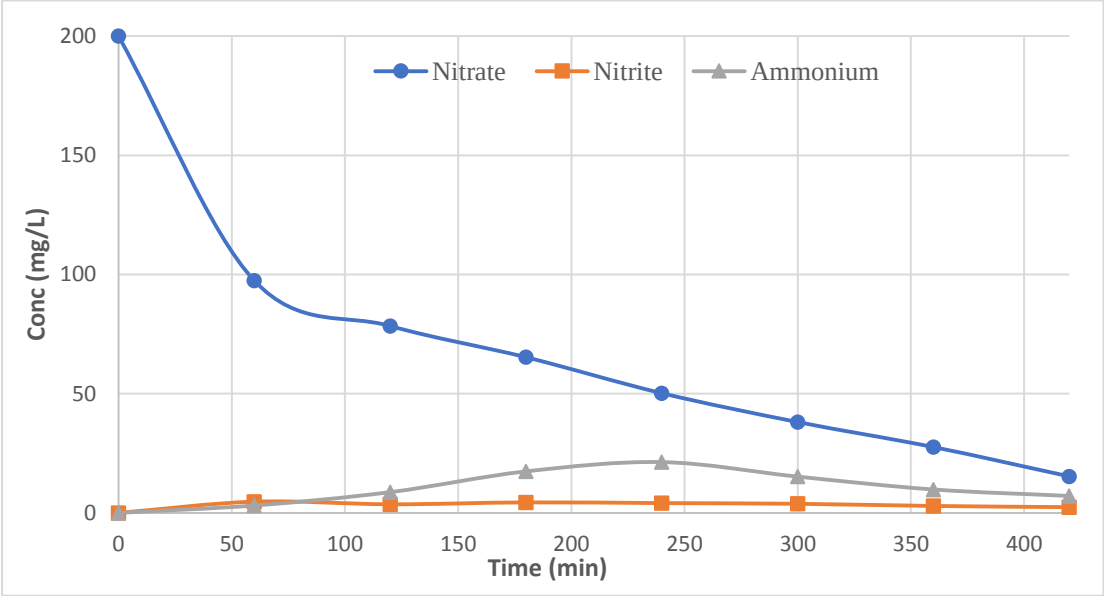

The working solution's nitrate content had reached 15.3 mg/L only after 420 minutes of electrolysis. The observed concentration falls below the permissible nitrate content as stipulated by the World Health Organization (50 mg/L). Approximately 92.35% of nitrate underwent conversion following the process of electrolysis. The concentration of nitrite in the working solution remained constant with slight variations during the course of the 420-minute electrolysis experiment, with a final measurement of 2.4 mg/L. The ammonium ion concentration exhibited an unexpected increase to 21.3 mg/L after 240 minutes of electrolysis, followed by a subsequent decline to 7.1 mg/L after 420 minutes of electrolysis.

Table 3.7

*Selectivity for byproducts (nitrite, ammonium, or dinitrogen gas) on Cu@Cu-1. All experiments were conducted by means of (80 mL; 0.05 M Na_2SO_4 + 200 mg/L NO_3^-, 25±**1**℃, and -1.80 V vs. SCE and different time intervals of electrolysis (120 min, 240 min, and 420 min)*

Time (min)	$[NO_3^-]$ $Conversion$ % (Based on mg L^- Conc.)	S% (Based on molar Conc.)		
		NO_2^-	NH_4^+	N_2
120	60.80	3.99	24.59	71.42
240	74.90	3.69	48.87	47.44
420	92.35	1.75	13.20	85.05

The selectivity of nitrogen rises when the electrolysis period is extended, as indicated in Table 3.7. The selectivity for ammonium upon 420 minutes of electrolysis was 13.20%, whereas the selectivity for nitrogen was 85.05%. The observed significant selectivity towards nitrogen gas serves as additional evidence supporting the successful application of our novel modified electrode Cu@Cu-1.

The electroreduction of nitrate ions is a reaction of considerable complexity known to proceed through a system of reactions (66). The process of nitrate electroreduction necessitates a primary adsorption phase wherein nitrate molecules are bound to the surface of the working electrode (110). The optimization of mass transfer and cathode surface area is crucial in order to enhance the effectiveness of nitrate electroreduction, as indicated by various studies (83,111,112). This finding substantiates one of the fundamental hypotheses in the present study regarding the newly developed Cu@Cu-1 electrode.

One phase in the process involves the adsorption of nitrate ions onto the surface of the electrode. Subsequently, an electron transfer process takes place, resulting in the formation of nitrite (NO_2^-) (110). Nitrate undergoes diverse pathways of reaction, resulting in the formation of different products such as nitrogen gas, ammonia, or different by-products (74,87).

Nitrite is the main semi-stable intermediate in the electrocatalytic reduction of nitrate. Figure 3.9 shows nitrite concentration variation, confirming its intermediate status. The nitrite compound has the potential to produce ammonia through many intermediates,

ultimately resulting in the formation of nitrogen (113). The integrated formulation of these laws can be found in equations 3.5, 3.6, and 3.7, as referenced in literature (114,115).

3.4.5 Variation of Alkalinity Throughout the Process

The pH variations of the working solutions over the course of 300 minutes of electrolysis are depicted in Figure A.10. The clearly apparent rise in pH can be attributed to the formation of hydroxyl groups, which is the outcome of the nitrate being converted to nitrite, ammonia, and nitrogen (108,116). The pH value demonstrates an upward trend during the duration of the process, reaching a stable level of approximately 11 ± 2 after 140 minutes of electrolysis.

3.4.6 Effect of Initial Nitrate Concentration

Using potentiostatic electrolysis at -1.80 V to determine the effect of increasing the initial nitrate concentration from 200 mg/L to 600 mg/L and 1000 mg/L, the nitrate removal amounts obtained were as follows: (121.61 mg, 60.8%), (267.60 mg, 44.6%), and (312.30 mg, 31.23%), respectively, as shown in Figure A.11. While the conversion percentage decreases with increasing nitrate concentration, there is a slight increase in absolute removal between 600 and 1000 nitrate concentration values, with 1000 demonstrating a slightly more pronounced decrease than 600. This illustrates the feasibility of the research in addressing the issue of nitrate contamination in water sources.

3.4.7 Stability and Reuse of Electrode

Using just one Cu@Cu-1 electrode, Figure A.12 displays the results of three consecutive potentiostatic electroreduction tests conducted at -1.80 V. The figure shows that in all three trials, the percentage of nitrate reduction was almost identical (60.8 ± 3%), achieved by using the same electrode for two hours. This indicates that the modified electrode (Cu@Cu-1) is efficient and stable.

3.4.8 Kinetics of Nitrate Reduction

The exploration of both rate order, as well as rate constant for the electrocatalytic process of nitrate removal on a Cu@Cu-1 electrode, was conducted by employing well-established integrated rate laws. The experimental data underwent analysis utilizing the

principles of the zero, first, and second-order kinetic models. The integrated formulation of these laws can be found in equations 3.5, 3.6, and 3.7, as referenced in the literature (114,115).

$$Zero\ Order: [C]_t = -Kt + [C]_0 \quad \ldots\ldots\ldots\ldots\ldots\ldots (3.5)$$

$$First\ Order: ln[C]_t = -Kt + ln\,[C]_0 \quad \ldots\ldots\ldots\ldots\ldots\ldots (3.6)$$

$$Second\ Order: \frac{1}{[C]_t} = Kt + \frac{1}{[C]_0} \quad \ldots\ldots\ldots\ldots\ldots\ldots (3.7)$$

In this context, $[C]_0$ represents the starting molar concentration of nitrate, $[C]_t$ represents the molar concentration of nitrate at a specific time (min), and k is the rate constant. To assess the suitability of the zero, first, and second-rate laws, linear plots were employed to examine the correlation between $[C]_t$ vs t, ln $[C]_t$ vs. t, and $1/[C]_t$ vs. t respectively. If any of these models is deemed acceptable, it is expected to exhibit a linear relationship, enabling the determination of the rate constant and their corresponding correlation coefficients (R^2).

The findings from the examinations conducted on the models pertaining to the electroreduction of nitrate on the Cu@Cu-1 electrode are presented in Figure A.13 (a, b, and c).

The coefficients of correlation for the models of zero-order, first-order, and second-order were found to be 0.87, 0.92, and 0.96, in that order. Thus, the values of the correlation coefficient (R^2) for the second-order model appear to exceed slightly those obtained for the zero-order and first-order models.

This suggests that the first or second-order kinetic model may be more appropriate than the zero-order model for describing the kinetics of electrochemical nitrate reduction. Nevertheless, there is no law that can be considered to be absolutely definitive due to the fact that the (R^2) values for the three alternative rate laws are not considerably different from one another.

An additional endeavor was undertaken to determine the rate order and constant by employing the approach of initial rate law, owing to the slight differences observed in the (R^2) values of the three rate laws (117). The study involved conducting three

electroreduction experiments with varying initial nitrate concentrations (200 mg/L, 600 mg/L, and 800 mg/L). The reaction rate generic formula is provided in equation (3.8) (118).

$$Rate_{initial} = k\,[C]_o^{n} \quad \ldots\ldots\ldots\ldots\ldots\ldots\ldots\ldots\ldots\ldots (3.8)$$

The application of natural logarithms to the two sides of equation (3.8) (118) results in:

$$\ln Rate_{initial} = \ln k + n\ln [C]_o \quad \ldots\ldots\ldots\ldots\ldots\ldots (3.9)$$

The variable n represents the order of the reaction. The initial rates for three distinct trials, each with varying initial nitrate concentrations, were determined. Plotting the nitrate concentration vs. time result yields a curve whose initial rate is equal to the slope of a tangent at the starting point (Figure A.14). Based on the data presented in Figure A.15, the relationship between ln Rate $_{initial}$ vs. ln $[C]_o$, was investigated. It was seen that the slope of the plot was determined to be 0.85, indicating that it is equivalent to the order of the reaction (n) when (n < 1). It is evident that nitrate is reduced and adsorbed at the electrode surface, along with the co-adsorption of other species (111). Furthermore, the value is similar to the ones depicted in the literature, as shown in Table 3.8. Additionally, the rate constant was determined by analyzing the intercept of the plot that is equal to ln k, from which k was found to = 1.39×10^{-2} min^{-1}.

Table 3.8

Comparative analysis of order and rate constant between Cu@Cu-1 electrode with reported literature

Electrode	Initial Nitrate Concentration	Order of the Reaction (n)	Rate Constant ($\times 10^{-4}$)	Area (cm^2)	Ref.
Cu/MWCNT/FTO	3.22×10^{-3} M	0.76	7.55 sec^{-1}	10	(88)
Cu/Graphite	1 M	0.88	0.75 sec^{-1}	4	(119)
Pd/Cu/Graphite	1 M	0.87	0.56 sec^{-1}	4	(119)
Cu@Cu-1	3.22×10^{-3} M	0.85	2.32 sec^{-1}	8	This Work

3.5 Comparative Analysis of Cu@Cu-1 with Literature

The effectiveness of this improved electrode in nitrate electroreduction was compared with other electrodes as described in Table 3.9. The results demonstrate the performance of the Cu@Cu-1 electrode in comparison to the findings reported in the literature. The primary selectivity reported in the literature for nitrate electroreduction by copper electrode was for ammonium, which reached 97% after 250 hours of electrolysis, with the remainder being nitrite (69). The Cu@Cu-1 electrode exhibited a nitrate removal efficiency of 92.35% within 7 hours, resulting in 13.2% NH_4^+ and 85.05% nitrogen. Our electrode exhibits superior efficiency and selectivity compared to existing reducing cathodes described in the literature. Compared to merely 7 hours here, lengthier periods of 250 hours were required in some literature to remove almost all of the nitrate (69).

The literature reports a maximum selectivity of nitrogen of 60-70%, attained by a bimetallic catalyst consisting of Cu and Pd during an electrolysis process that lasted approximately 48 hours (119). In contrast, the Cu@Cu-1 catalyst produced a selectivity of 85.05% for nitrogen in just 7 hours of electrolysis. Hence, the catalyst outlined in this context exhibits superior efficiency and selectivity in comparison to alternative options.

These findings indicate that the Cu@Cu-1 electrode is highly recommended for the purpose of removing nitrates from aqueous solutions. Furthermore, the electrolytic system employed in this study was uncomplicated, and the electrolyte utilized was non-toxic, in contrast to those described in existing literature. In addition to these benefits, it is worth mentioning that the required operating potential in our catalyst is nothing more than -1.80 V.

Table 3.9

Comparison between Cu@Cu-1 and electrodes reported in the literature

Operation & Configuration	*Reaction Media*	*Electrode Material*			*Power Supply*	*Time*	*NO_3^- Conversion %*	*Final Products*			*Ref*
								S%			
		Cathode	*Anode*	*Reference*				*NH_4^+*	*NO_2^-*	*N_2*	
Two Compartment Cell Separated by Cationic Exchange Membrane	1 M NaOH + 0.1 M NO_3^-	Cu disk	Pt	Hg/HgO	-1.40 V	250 h	100	97	3	-	(69)
Batch Electrochemical Cell	0.1 M Na_2SO_4 + 3.6 g/L KNO_3	Ti/CNTs/Cu 5-Pd5	SCE	Hg/Hg_2Cl_2	-1.30 V	4 h	32.52	54.0	3.5	42.5	(85)
Batch Electrochemical Cell	1 M $NaNO_3$ + 0.5 M NaOH	Pd-Cu/Graphite	Pt	Hg/HgO	-1.10 V	48 h	100	1	29	70	(119)
Batch Electrochemical Cell	0.05 M Na_2SO_4 + 200 mg/L NO_3^-	Cu@Cu-1	Pt	SCE	-1.80 V	7 h	92.35%	13.2	1.75	80.05	This Work

Chapter Four

Conclusion

4.1 Conclusion

To reduce nitrates via electroreduction, various electrodes have been adjusted, characterized, and implemented. From this investigation, several conclusions were drawn:

1. The potentiostatic method of electrodeposition of Cu nanoparticles onto the copper surface improved the adhesion of the deposited layer and the Cu surface.
2. In this study, the thin coating of Cu nanoparticles on Cu electrodes demonstrated greater stability and nitrate reduction rates than other electrodes that were prepared.
3. Copper nanoparticles on copper sheet have demonstrated a high N_2 selectivity.
4. The Cu@Cu-1 electrode exhibited greater nitrate electroreduction efficiency than the Cu sheet, demonstrating the critical nature of Cu nanoparticles.
5. In this study, a Cu@Cu-1 electrode was effectively prepared for the first time.
6. N_2 was the primary product of nitrate electroreduction by the Cu@Cu-1 electrode following 7 hours of electrolysis.
7. As an electrode, the modified Cu@Cu-1 electrode demonstrated the most effective nitrate electroreduction performance and was utilized to investigate the impact of various parameters on nitrate electroreduction.
8. At modest overpotentials (E = -1.80 V vs. SCE), electrolysis with Cu@Cu-1 revealed a relatively rapid decrease in nitrate concentration, validating the electrode's elevated performance.
9. In a durability test, the Cu@Cu-1 electrode maintains stability and upholds its catalytic activity.

4.2 Future Proposals

It is advisable to perform a thorough investigation into the following:

1. Implementing Cu@Cu-1 electrode for nitrate electroreduction on real world samples extracted from ground water.
2. An effective approach to enhance the stability of the Cu@Cu-1 electrode is to optimize the reduction rate, as the observed results did not meet the expectations.

3. Investigating the process of nitrate reduction through the utilization of various counter electrodes.
4. Performing nitrate reduction studies utilizing various electrolyte compositions.
5. To preform a BET surface analysis to the Cu@Cu-1 electrode.

List of Abbreviations

Abbreviation	Meaning
SSA	Specific Surface Area
WHO	World health organization
LUMO	Lowest unoccupied molecular orbital
UV - VIS	Ultraviolet visible
NP	Nanoparticles
CV	Cyclic voltammetry
XPS	X-ray photoelectron spectroscopy
SEM	Scanning electron microscopy
EDS	Energy dispersive X-ray spectroscopy
XRD	X-ray diffraction
SCE	Saturated calomel electrode
S%	Selectivity percentage
R^2	Correlation coefficient

References

1. Stefanakis AI, Zouzias D, Marsellos A. Groundwater Pollution: Human and Natural Sources and Risks. Water Pollut. 4.

2. Baker B, Aldridge C, Omer A. Water: Availability and use. Miss State Univ Ext. 2016 Nov 1;2016:p3011.

3. Carrard N, Foster T, Willetts J. Groundwater as a Source of Drinking Water in Southeast Asia and the Pacific: A Multi-Country Review of Current Reliance and Resource Concerns. Water. 2019 Aug;11(8):1605.

4. Velis M, Conti KI, Biermann F. Groundwater and human development: synergies and trade-offs within the context of the sustainable development goals. Sustain Sci. 2017 Nov 1;12(6):1007–17.

5. Khatun R. Water Pollution: Causes, Consequences, Prevention Method and Role of WBPHED with Special Reference from Murshidabad District. 2017;7(8).

6. Talabi AO, Kayode TJ. Groundwater Pollution and Remediation. J Water Resour Prot. 2019;11(01):1–19.

7. Smith RL, Howes BL, Duff JH. Denitrification in nitrate-contaminated groundwater: Occurrence in steep vertical geochemical gradients. Geochim Cosmochim Acta. 1991 Jul;55(7):1815–25.

8. Almasri MN. Nitrate contamination of groundwater: A conceptual management framework. Environ Impact Assess Rev. 2007 Apr;27(3):220–42.

9. Stein LY, Klotz MG. The nitrogen cycle. Curr Biol. 2016 Feb;26(3):R94–8.

10. Francis CA, Beman JM, Kuypers MMM. New processes and players in the nitrogen cycle: the microbial ecology of anaerobic and archaeal ammonia oxidation. ISME J. 2007 May;1(1):19–27.

11. Widdison PE, Burt TP. Nitrogen Cycle. In: Encyclopedia of Ecology [Internet]. Elsevier; 2008 [cited 2023 Feb 20]. p. 2526–33. Available from: https://linkinghub.elsevier.com/retrieve/pii/B9780080454054007503

12. Smil V. Nitrogen in crop production: An account of global flows. Glob Biogeochem Cycles. 1999 Jun;13(2):647–62.

13. Galloway JN, Aber JD, Erisman JW, Seitzinger SP, Howarth RW, Cowling EB, et al. The Nitrogen Cascade. BioScience. 2003 Apr 1;53(4):341–56.

14. Galloway J, Dentener F, Boyer E, Howarth R, Seitzinger S, Asner G, et al. Nitrogen Cycles: Past, Present, and Future. Biogeochemistry. 2004 Jan 9;70:153–226.

15. Watson SW, Valois FW, Waterbury JB. The Family Nitrobacteraceae. In: Starr MP, Stolp H, Trüper HG, Balows A, Schlegel HG, editors. The Prokaryotes [Internet]. Berlin, Heidelberg: Springer Berlin Heidelberg; 1981 [cited 2023 Feb 26]. p. 1005–22. Available from: http://link.springer.com/10.1007/978-3-662-13187-9_80

16. Skiba U. Denitrification. In: Encyclopedia of Ecology [Internet]. Elsevier; 2008 [cited 2023 Feb 26]. p. 866–71. Available from: https://linkinghub.elsevier.com/retrieve/pii/B9780080454054002640

17. Ward BB. Nitrification and denitrification: Probing the nitrogen cycle in aquatic environments. Microb Ecol [Internet]. 1996 Nov [cited 2023 Feb 26];32(3). Available from: http://link.springer.com/10.1007/BF00183061

18. Smil V. Nitrogen cycle and world food production.

19. Afzal BM. Drinking water and women's health. J Midwifery Womens Health. 2006;51(1):12–8.

20. Abdallah R, Geneste F, Labasque T, Djelal H, Fourcade F, Amrane A, et al. Selective and quantitative nitrate electroreduction to ammonium using a porous copper electrode in an electrochemical flow cell. J Electroanal Chem. 2014 Aug;727:148–53.

21. World Health Organization. Nitrate and nitrite in drinking-water: background document for development of WHO guidelines for drinking-water quality [Internet]. World Health Organization; 2003 [cited 2023 May 20]. Report No.:

WHO/SDE/WSH/04.03/56. Available from: https://apps.who.int/iris/handle/10665/75380

22. Anayah FM, Almasri MN. Trends and occurrences of nitrate in the groundwater of the West Bank, Palestine. Appl Geogr. 2009 Dec;29(4):588–601.

23. Grabda E, Einszporn-Orecka T, Felińska C, Zbanyszek R. Experimental methemoglobinemia in rainbow trout [Internet]. Pensoft Publishers; 1974 [cited 2023 Mar 27]. Available from: https://doaj.org/article/f2244e12d77d468a9c1b514636d4e98b

24. Lijinsky W. N-Nitroso compounds in the diet. Mutat Res. 1999 Jul 15;443(1–2):129–38.

25. Ward MH, Jones RR, Brender JD, de Kok TM, Weyer PJ, Nolan BT, et al. Drinking Water Nitrate and Human Health: An Updated Review. Int J Environ Res Public Health. 2018 Jul;15(7):1557.

26. World Health Organization. Guidelines for drinking-water quality. 4th ed. 2011 [cited 2023 Jul 20]; Available from: https://apps.who.int/iris/handle/10665/44584

27. Ferro S. Removal of nitrates from highly-contaminated industrial wastewater. Chim E L'Industria Milan Italy. 2012 Mar 1;94:100–10.

28. Clifford DA. Ion exchange and inorganic adsorption. MCGRAW-HILL INCUSA 1194. 1990;1990.

29. Clifford DA, Weber WJ. A Nitrate-Removal Ion-Exchange Process With a Land-Disposable Regenerant. In: Proceedings of the 1977 National Conference on Treatment and Disposal of Industrial Wastewaters and Residues April 26-28, 1977, Houston, Texas, p 216-225, 1977 10 fig, 4 tab, 16 ref. 1977.

30. Rautenbach R, Kopp W, van Opbergen G, Hellekes R. Nitrate reduction of well water by reverse osmosis and electrodialysis - studies on plant performance and costs. Desalination. 1987 Nov 1;65:241–58.

31. Panyor L, Fabiani C. Anion rejection in a nitrate highly rejecting reverse osmosis thin-film composite membrane. Desalination. 1996 May 1;104(3):165–74.

32. Mani KN. Electrodialysis water splitting technology. J Membr Sci. 1991 May 15;58(2):117–38.

33. Aghapour AA, Nemati S, Mohammadi A, Nourmoradi H, Karimzadeh S. Nitrate removal from water using alum and ferric chloride: A comparative study of alum and ferric chloride efficiency. Environ Health Eng Manag. 2016 Mar 26;3(2):69–73.

34. Mikuška P, Večeřa Z. Simultaneous determination of nitrite and nitrate in water by chemiluminescent flow-injection analysis. Anal Chim Acta. 2003 Oct 24;495(1):225–32.

35. Matějů V, Čižinská S, Krejčí J, Janoch T. Biological water denitrification—A review. Enzyme Microb Technol. 1992 Mar 1;14(3):170–83.

36. Ghafari S, Hasan M, Aroua MK. Bio-electrochemical removal of nitrate from water and wastewater--a review. Bioresour Technol. 2008 Jul;99(10):3965–74.

37. Gao W, Guan N, Chen J, Guan X, Jin R, Zeng H, et al. Titania supported Pd-Cu bimetallic catalyst for the reduction of nitrate in drinking water. Appl Catal B Environ. 2003 Nov;46(2):341–51.

38. Inazu K, Kitahara M, Aika K ichi. Decomposition of ammonium nitrate in aqueous solution using supported platinum catalysts. Catal Today. 2004 Sep 1;93–95:263–71.

39. Ottley CJ, Davison W, Edmunds WM. Chemical catalysis of nitrate reduction by iron (II). Geochim Cosmochim Acta. 1997 May 1;61(9):1819–28.

40. Pletcher D, Walsh FC. Industrial Electrochemistry [Internet]. Dordrecht: Springer Netherlands; 1993 [cited 2023 Jul 17]. Available from: http://link.springer.com/10.1007/978-94-011-2154-5

41. Panizza M, Michaud PA, Cerisola G, Comninellis C, editors. Electrochemical treatment of wastewaters containing organic pollutants on boron-doped diamond electrodes: Prediction of specific energy consumption and required electrode area. Electrochem Commun. 2001;

42. Kaczur J, Cawlfield D. Oxyhalide and Oxynitrogen Specie Removal from Aqueous Solutions by Electrochemical Reduction. In 1994.

43. Kaczur JJ, Cawlfield DW, Woodard KE. Process and apparatus for the removal of oxyhalide species from aqueous solutions [Internet]. US5167777A, 1992 [cited 2023 Jul 10]. Available from: https://patents.google.com/patent/US5167777/en

44. Xu D, Li Y, Yin L, Ji Y, Niu J, Yu Y. Electrochemical removal of nitrate in industrial wastewater. Front Environ Sci Eng. 2018 Feb 15;12(1):9.

45. Bosko ML, Rodrigues MAS, Ferreira JZ, Miró EE, Bernardes AM. Nitrate reduction of brines from water desalination plants by membrane electrolysis. J Membr Sci. 2014 Feb 1;451:276–84.

46. Dash BP, Chaudhari S. Electrochemical denitrificaton of simulated ground water. Water Res. 2005 Oct 1;39(17):4065–72.

47. Li M, Feng C, Zhang Z, Shen Z, Sugiura N. Electrochemical reduction of nitrate using various anodes and a Cu/Zn cathode. Electrochem Commun - ELECTROCHEM COMMUN. 2009 Oct 1;11:1853–6.

48. Sa YJ, Lee CW, Lee SY, Na J, Lee U, Hwang YJ. Catalyst–electrolyte interface chemistry for electrochemical CO2 reduction. Chem Soc Rev. 2020 Sep 21;49(18):6632–65.

49. Polatides C, Kyriacou G. Electrochemical reduction of nitrate ion on various cathodes – reaction kinetics on bronze cathode. J Appl Electrochem. 2005 May 1;35(5):421–7.

50. Xiang Y, Zhou DL, Rusling JF. Electrochemical conversion of nitrate to ammonia in water using cobalt-DIM as catalyst. J Electroanal Chem. 1997 Mar 15;424(1):1–3.

51. Chebotareva N, Nyokong T. Metallophthalocyanine catalysed electroreduction of nitrate and nitrite ions in alkaline media. J Appl Electrochem. 1997 Aug 1;27(8):975–81.

52. BOCKRIS JO, KIM J. Electrochemical treatment of low-level nuclear wastes. J Appl Electrochem. 1997 Jun 1;27(6):623–34.

53. Paidar M, Roušar I, Bouzek K. Electrochemical removal of nitrate ions in waste solutions after regeneration of ion exchange columns. J Appl Electrochem. 1999 May 1;29(5):611–7.

54. Küngas R. Review—Electrochemical CO2 Reduction for CO Production: Comparison of Low- and High-Temperature Electrolysis Technologies. J Electrochem Soc. 2020 Feb;167(4):044508.

55. Holze R. Book Review: Electrochemical Methods. Fundamentals and Applications (2nd Edition). By Allen J. Bard and Larry R. Faulkner. Angew Chem Int Ed. 2002;41(4):655–7.

56. Vetter KJ. Electrochemical Kinetics: Theoretical Aspects. Elsevier; 2013. 488 p.

57. Huang H, Zhao M, Xing X, Bae IT, Scherson D. In-situ infrared studies of the Cd-UPD mediated reduction of nitrate on gold. J Electroanal Chem Interfacial Electrochem. 1990 Oct 25;293(1):279–84.

58. Rivera FF, de León CP, Nava JL, Walsh FC. The filter-press FM01-LC laboratory flow reactor and its applications. Electrochimica Acta. 2015 May 1;163:338–54.

59. Paidar M, Bouzek K, Bergmann H. Influence of cell construction on the electrochemical reduction of nitrate. Chem Eng J. 2002 Jan 28;85(2):99–109.

60. Abuzaid NS, Al-Hamouz Z, Bukhari AA, Essa MH. Electrochemical Treatment of Nitrite Using Stainless Steel Electrodes. Water Air Soil Pollut. 1999 Jan 1;109(1):429–42.

61. Hsieh SJ, Gewirth AA. Nitrate Reduction Catalyzed by Underpotentially Deposited Cd on Au(111): Identification of the Electroactive Surface Structure. Langmuir. 2000 Nov 1;16(24):9501–12.

62. da Cunha MCPM, Weber M, Nart FC. On the adsorption and reduction of NO3− ions at Au and Pt electrodes studied by in situ FTIR spectroscopy. J Electroanal Chem. 1996 Jan 1;414(2):163–70.

63. G. Casella I, Contursi M. Highly dispersed rhodium particles on multi-walled carbon nanotubes for the electrochemical reduction of nitrate and nitrite ions in acid medium. Electrochimica Acta. 2014 Aug 20;138:447–53.

64. Cuibus F, Ispas A, Bund A, Ilea P. Square wave voltammetric detection of electroactive products resulting from electrochemical nitrate reduction in alkaline media. J Electroanal Chem. 2012 Jun 1;675:32–40.

65. Wang L, Li M, Liu X, Feng C, Zhou F, Chen N, et al. Mechanism and Effectiveness of Ti-based Nano-Electrode for Electrochemical Denitrification. Int J Electrochem Sci. 2017;12.

66. de Groot MT, Koper MTM. The influence of nitrate concentration and acidity on the electrocatalytic reduction of nitrate on platinum. J Electroanal Chem. 2004 Jan 15;562(1):81–94.

67. Dima GE, Beltramo GL, Koper MTM. Nitrate reduction on single-crystal platinum electrodes. Electrochimica Acta. 2005 Aug 1;50(21):4318–26.

68. Bard AJ. Standard Potentials in Aqueous Solution. New York: Routledge; 2017. 848 p.

69. Reyter D, Bélanger D, Roué L. Study of the electroreduction of nitrate on copper in alkaline solution. Electrochimica Acta. 2008 Aug 1;53:5977–84.

70. De Francesco M, Costamagna P. On the design of electrochemical reactors for the treatment of polluted water. J Clean Prod. 2004 Mar 1;12(2):159–63.

71. Reyter D, Bélanger D, Roué L. Optimization of the cathode material for nitrate removal by a paired electrolysis process. J Hazard Mater. 2011 Aug 30;192(2):507–13.

72. Meng S, Ling Y, Yang M, Zhao X, Osman AI, Al-Muhtaseb AH, et al. Recent research progress of electrocatalytic reduction technology for nitrate wastewater: A review. J Environ Chem Eng. 2023 Apr;11(2):109418.

73. Haque I, Tariq M. Electrochemical reduction of nitrate: a review. J- Chem Soc Pak. 2010 Jan 1;32:396–418.

74. Kaczur J. Electrochemical Reduction of Nitrate. In 1998.

75. Gootzen JFE, Lefferts L, van Veen JAR. Electrocatalytic nitrate reduction on palladium based catalysts activated with germanium. Appl Catal Gen. 1999 Nov 5;188(1):127–36.

76. Li H lin, Robertson DH, Chambers JQ, Hobbs DT. Electrochemical Reduction of Nitrate and Nitrite in Concentrated Sodium Hydroxide at Platinum and Nickel Electrodes. J Electrochem Soc. 1988 May 1;135(5):1154.

77. Janssen LJJ, Pieterse MMJ, Barendrecht E. Reduction of nitric oxide at a platinum cathode in an acidic solution. Electrochimica Acta. 1977 Jan 1;22(1):27–30.

78. Dortsiou M, Katsounaros I, Polatides C, Kyriacou G. Electrochemical removal of nitrate from wastewaters on a zinc cathode. In 2009.

79. Seetharam B, Thallapalli B, Basha U, Murthy H, Kalkur J, Kumar S, et al. Effect of Operational Parameters on Nitrate Removal from the Simulated Groundwater Using Electrochemical Method. Int J Trend Res Dev. 2016 Jan 22;3:131–9.

80. Cattarin S. Electrochemical reduction of nitrogen oxyanions in 1 M sodium hydroxide solutions at silver, copper and CuInSe2 electrodes. J Appl Electrochem. 1992 Nov 1;22(11):1077–81.

81. Aouina N, Cachet H, Debiemme-chouvy C, Tran TTM. Insight into the electroreduction of nitrate ions at a copper electrode, in neutral solution, after determination of their diffusion coefficient by electrochemical impedance spectroscopy. Electrochimica Acta. 2010 Oct 1;55(24):7341–5.

82. González Pérez O, Bisang JM. Removal of nitrate using an activated rotating cylinder electrode. Electrochimica Acta. 2016 Mar 10;194:448–53.

83. Lima AS, Salles MO, Ferreira TL, Paixão TRLC, Bertotti M. Scanning electrochemical microscopy investigation of nitrate reduction at activated copper cathodes in acidic medium. Electrochimica Acta. 2012 Sep 1;78:446–51.

84. Ehrenburg MR, Danilov AI, Botryakova IG, Molodkina EB, Rudnev AV. Electroreduction of nitrate anions on cubic and polyoriented platinum

nanoparticles modified by copper adatoms. J Electroanal Chem. 2017 Oct 1;802:109–17.

85. Zhang Q, Ding L, Cui H, Zhai J, Wei Z, Li Q. Electrodeposition of Cu-Pd alloys onto electrophoretic deposited carbon nanotubes for nitrate electroreduction. Appl Surf Sci. 2014 Jul 30;308:113–20.

86. Mattarozzi L, Cattarin S, Comisso N, Gambirasi A, Guerriero P, Musiani M, et al. Hydrogen evolution assisted electrodeposition of porous Cu-Ni alloy electrodes and their use for nitrate reduction in alkali. Electrochimica Acta. 2014 Sep 1;140:337–44.

87. Yang S, Wang L, Jiao X, Li P. Electrochemical Reduction of Nitrate on Different Cu-Zn Oxide Composite Cathodes. Int J Electrochem Sci. 2017 Feb;12(5):4370–83.

88. Nassar H, Zyoud A, Helal HHS, Kim TW, Hilal HS. Effective and selective electroreduction of aqueous nitrate catalyzed by copper particles on multi-walled carbon nanotubes. J Environ Manage. 2022 Mar 1;305:114420.

89. Mattarozzi L, Cattarin S, Comisso N, Gerbasi R, Guerriero P, Musiani M, et al. Electrodeposition of compact and porous Cu-Pd alloy layers and their application to nitrate reduction in alkali. Electrochimica Acta. 2017 Mar 10;230:365–72.

90. Casella I, Contursi M. An electrochemical and XPS study of the electrodeposited binary Pd–Sn catalyst: The electroreduction of nitrate ions in acid medium. J Electroanal Chem - J ELECTROANAL CHEM. 2006 Mar 1;588:147–54.

91. Nassar HNI. Reduction of Nitrate Ion from Water using Nano-Copper Based Electrocatalyst.

92. Bridgewater L, Association APH, Association AWW, Federation WE. Standard Methods for the Examination of Water and Wastewater. American Public Health Association; 2012. 724 p.

93. Mutlu R, Yazici B. Copper-deposited aluminum anode for aluminum-air battery. J Solid State Electrochem. 2019 Feb 1;23.

94. Çakır O, Temel H, Kiyak M. Chemical etching of Cu-ETP copper. J Mater Process Technol. 2005 May 15;162–163:275–9.

95. Tessonnier JP, Barteau MA. Dispersion of Alkyl-Chain-Functionalized Reduced Graphene Oxide Sheets in Nonpolar Solvents. Langmuir. 2012 Apr 24;28(16):6691–7.

96. Warren BE. X-ray diffraction [Internet]. Dover ed. New York: Dover Publications; 1990 [cited 2024 Apr 22]. 381 p. Available from: http://catdir.loc.gov/catdir/description/dover031/89078470.html

97. Standards USNB of. Standard X-ray Diffraction Powder Patterns. U. S. Department of Commerce, National Bureau of Standards; 1953. 806 p.

98. Otte HM. Lattice Parameter Determinations with an X-Ray Spectrogoniometer by the Debye-Scherrer Method and the Effect of Specimen Condition. J Appl Phys. 1961 Aug 1;32:1536–46.

99. Powell C. X-ray Photoelectron Spectroscopy Database XPS,Version 4.1, NIST Standard Reference Database 20 [Internet]. National Institute of Standards and Technology; 1989 [cited 2023 Apr 8]. Available from: http://srdata.nist.gov/xps/

100. Karimzadeh M, Niknam K, Manouchehri N, Tarokh D. A green route for the cross-coupling of azide anions with aryl halides under both base and ligand-free conditions: exceptional performance of a Cu $_2$ O–CuO–Cu–C nanocomposite. RSC Adv. 2018;8(45):25785–93.

101. Abdallah R, Geneste F, Labasque T, Djelal H, Fourcade F, Amrane A, et al. Selective and quantitative nitrate electroreduction to ammonium using a porous copper electrode in an electrochemical flow cell. J Electroanal Chem. 2014 Aug;727:148–53.

102. Soares OSGP, Órfão JJM, Pereira MFR. Nitrate reduction in water catalysed by Pd–Cu on different supports. Desalination. 2011 Sep;279(1–3):367–74.

103. De D, Englehardt JD, Kalu EE. Electroreduction of Nitrate and Nitrite Ion on a Platinum-Group-Metal Catalyst-Modified Carbon Fiber Electrode

Chronoamperometry and Mechanism Studies. J Electrochem Soc. 2000;147(12):4573.

104. Cheng H, Scott K, Christensen PA. Paired electrolysis in a solid polymer electrolyte reactor—Simultaneously reduction of nitrate and oxidation of ammonia. Chem Eng J. 2005 Apr 15;108(3):257–68.

105. Katsounaros I, Dortsiou M, Polatides C, Preston S, Kypraios T, Kyriacou G. Reaction pathways in the electrochemical reduction of nitrate on tin. Electrochimica Acta. 2012 Jun;71:270–6.

106. He Q, Tian Y, Wu Y, Liu J, Li G, Deng P, et al. Electrochemical Sensor for Rapid and Sensitive Detection of Tryptophan by a Cu2O Nanoparticles-Coated Reduced Graphene Oxide Nanocomposite. Biomolecules. 2019 May 8;9(5):176.

107. Long J, Dong J, Wang X, Ding Z, Zhang Z, Wu L, et al. Photochemical synthesis of submicron- and nano-scale Cu2O particles. J Colloid Interface Sci. 2009 May 15;333(2):791–9.

108. Talhi B, Monette F, Azzouz A. Effective and selective nitrate electroreduction into nitrogen through synergistic parameter interactions. Electrochimica Acta. 2011 Dec 30;58:276–84.

109. Huang W, Li M, Zhang B, Feng C, Lei X, Xu B. Influence of operating conditions on electrochemical reduction of nitrate in groundwater. Water Environ Res Res Publ Water Environ Fed. 2013 Mar;85(3):224–31.

110. Amatore C, Saveant JM. Do ECE mechanisms occur in conditions where they could be characterized by electrochemical kinetic techniques? J Electroanal Chem Interfacial Electrochem. 1978 Jan 10;86(1):227–32.

111. Dima GE, de Vooys ACA, Koper MTM. Electrocatalytic reduction of nitrate at low concentration on coinage and transition-metal electrodes in acid solutions. J Electroanal Chem. 2003 Sep 15;554–555:15–23.

112. Katsounaros I, Kyriacou G. Influence of the concentration and the nature of the supporting electrolyte on the electrochemical reduction of nitrate on tin cathode. Electrochimica Acta. 2007 Jul 10;52(23):6412–20.

113. Vavilin VA, Rytov SV. Nitrate denitrification with nitrite or nitrous oxide as intermediate products: Stoichiometry, kinetics and dynamics of stable isotope signatures. Chemosphere. 2015 Sep 1;134:417–26.

114. Lee J. Reaction Order Ambiguity in Integrated Rate Plots. J Chem Educ. 2008 Jan;85(1):141–4.

115. Makover J, Hasson D, Huang Y, Semiat R, Shemer H. Electrochemical removal of nitrate from a Donnan dialysis waste stream. Water Sci Technol. 2019 Sep 12;80(4):727–36.

116. Durivault L, Brylev O, Reyter D, Sarrazin M, Bélanger D, Roué L. Cu–Ni materials prepared by mechanical milling: Their properties and electrocatalytic activity towards nitrate reduction in alkaline medium. J Alloys Compd. 2007 Apr 1;432:323–32.

117. Ryan MAndrieu, Ingle JD. Fluorometric reaction rate method for the determination of thiamine. Anal Chem. 1980 Nov 1;52(13):2177–84.

118. Justi R. Teaching and Learning Chemical Kinetics. In: Gilbert JK, De Jong O, Justi R, Treagust DF, Van Driel JH, editors. Chemical Education: Towards Research-based Practice [Internet]. Dordrecht: Springer Netherlands; 2003 [cited 2023 Sep 18]. p. 293–315. (Science & Technology Education Library). Available from: https://doi.org/10.1007/0-306-47977-X_13

119. Ghodbane O, Sarrazin M, Roué L, Bélanger D. Electrochemical Reduction of Nitrate on Pyrolytic Graphite-Supported Cu and Pd–Cu Electrocatalysts. J Electrochem Soc - J ELECTROCHEM SOC. 2008 Jan 1;155.

Appendices

Appendix A

Figure

Figure A.1

Measured XRD pattern for (a) Cu@Cu-1 and (b) Used Cu@Cu-1.

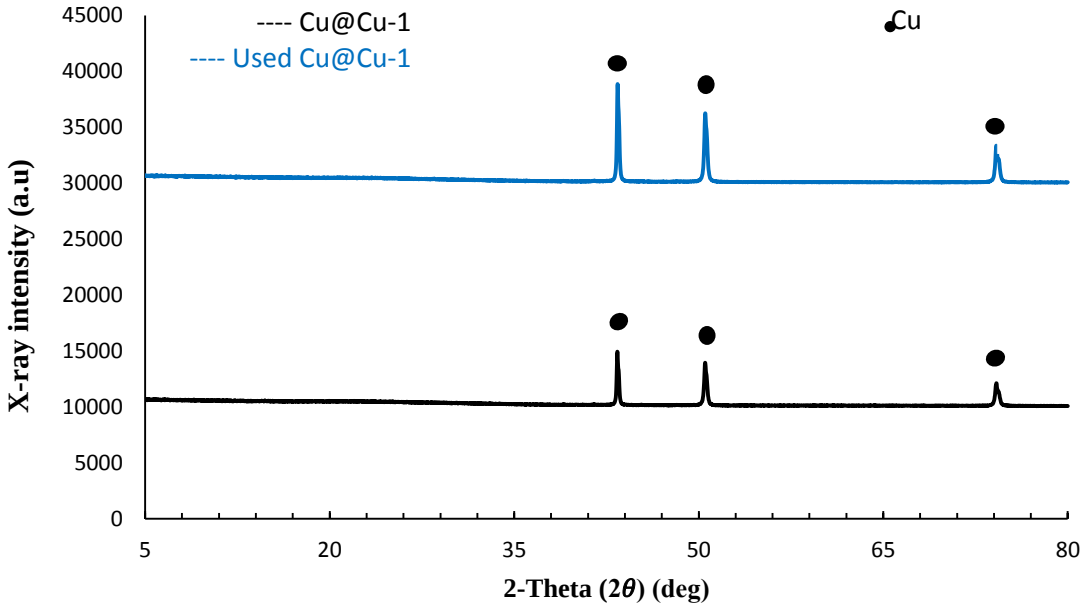

Figure A.2

XPS spectra of used Cu@Cu-1, (a) Complete spectra, (b) Cu 2p peak, and (c) O 1s peak.

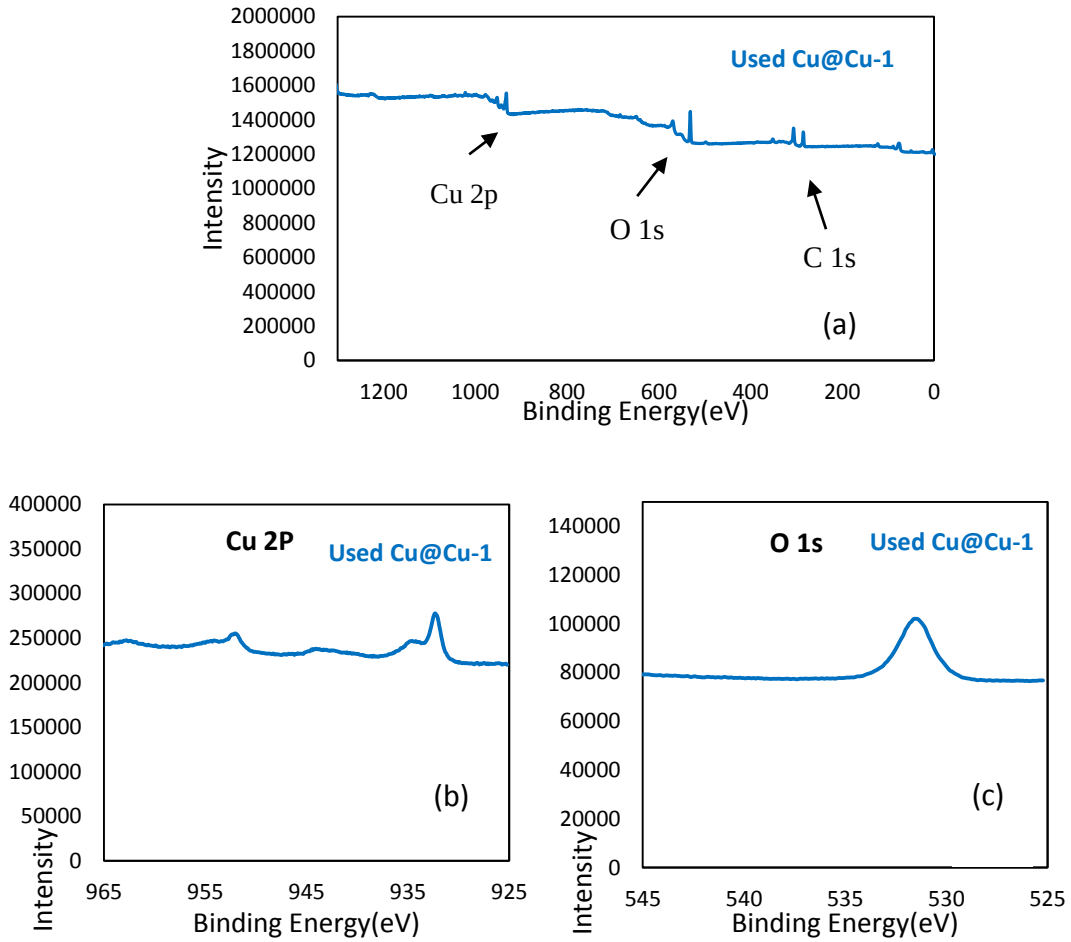

Figure A.3

Cyclic voltammogram on Cu -1 in 0.05 M Na_2SO_4 and in (0.05 M Na_2SO_4 + 200 mg/L NO_3^{-})

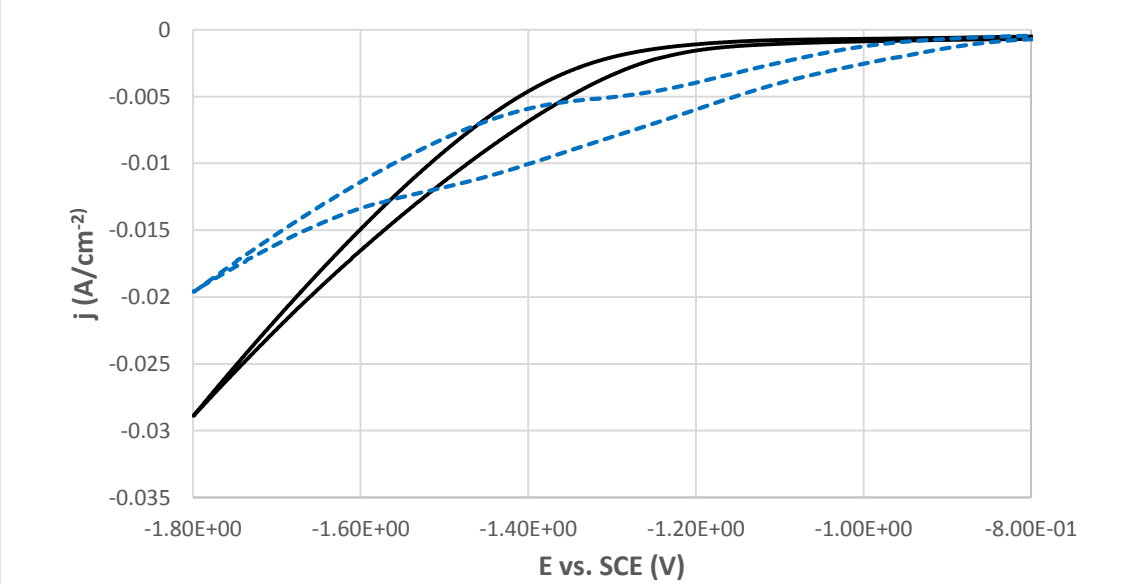

Figure A.4

Measured XRD pattern for Etched Cu-2

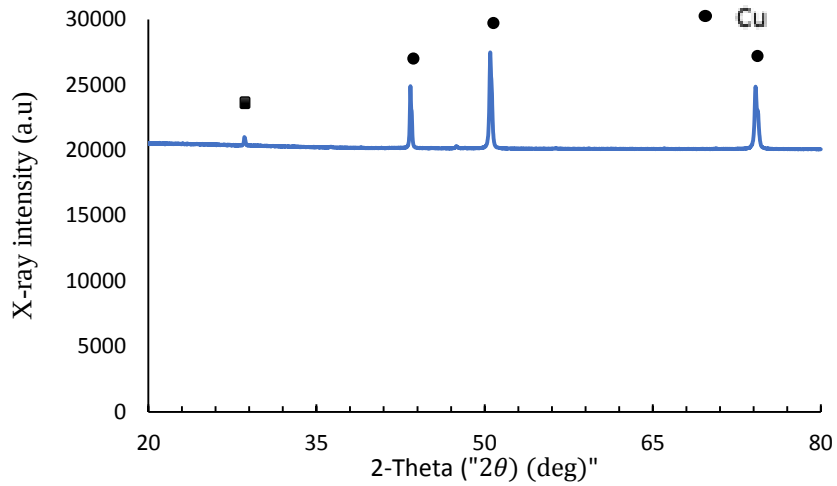

Figure A.5

XPS spectra of Cu-2, (a) Complete spectra, (b) Cu 2p peak, and (c) O 1s peak.

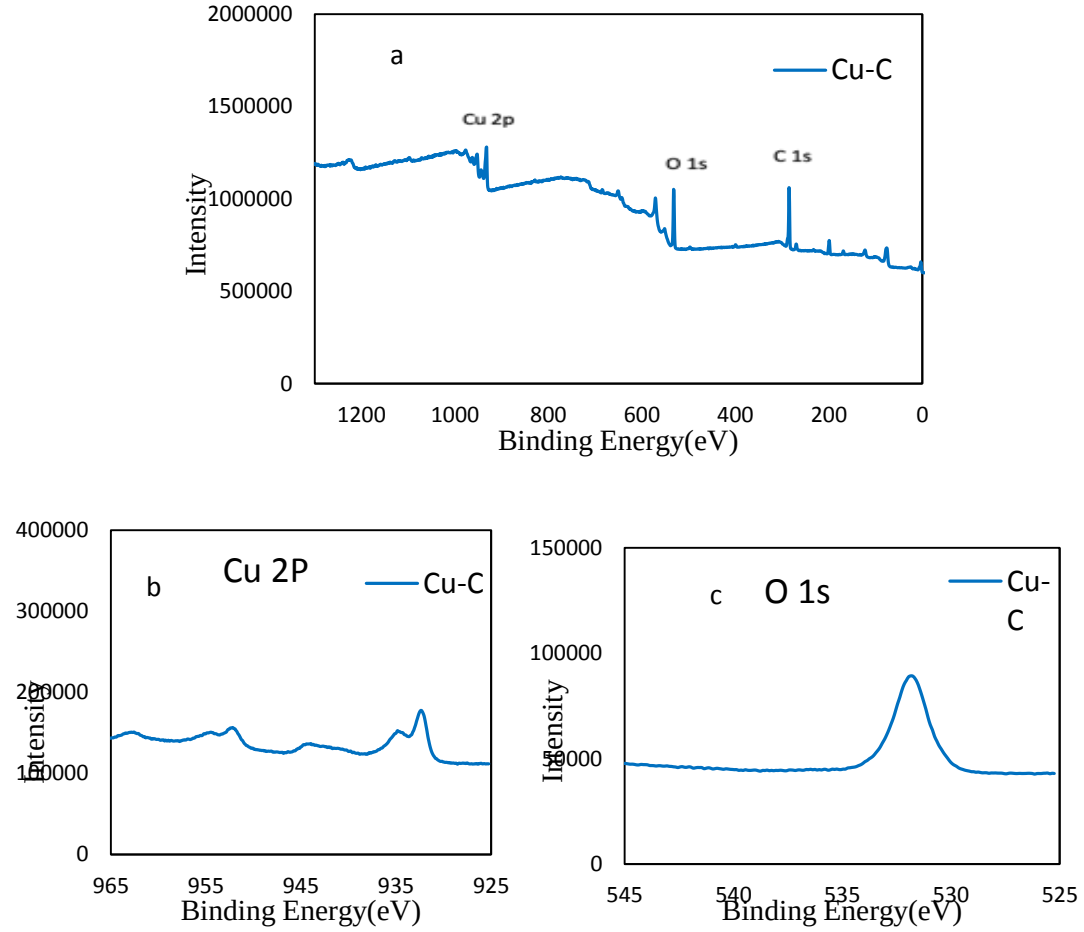

Figure A.6

Cyclic voltammogram on Etched Cu -2 in ~~0.05~~M Na_2SO_4 and in (~~0.05~~ M Na_2SO_4 + 200 mg/L NO_3^{-})

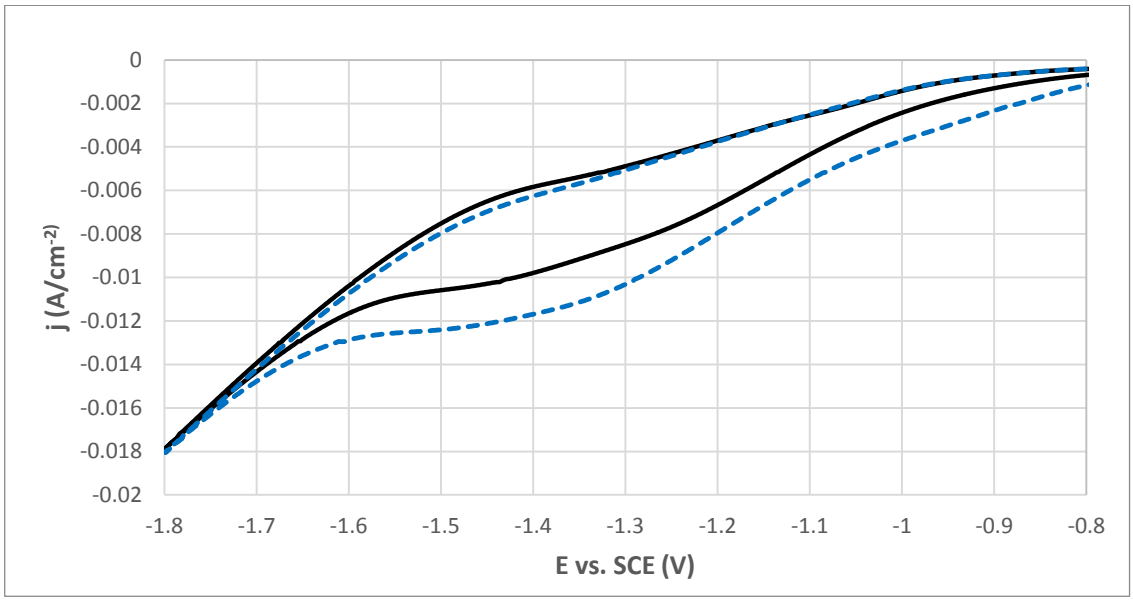

Figure A.7

Nitrate, nitrite, and ammonium concentrations vs. electrolysis time by Etched Cu-2 modified electrode. All experiments were conducted by means of (80 mL; 0.05 M Na_2SO_4 + 200 mg/L NO_3^{-}), 120 min, 25 ± 1℃, and -1.80 V vs. SCE.

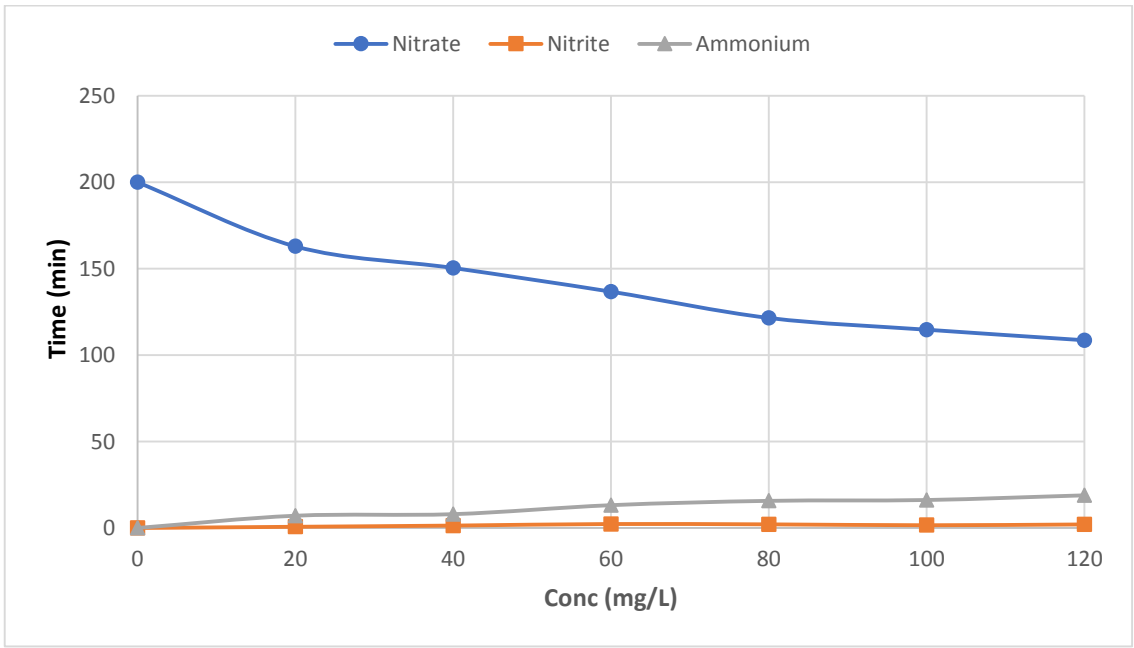

Figure A.8

Nitrate conversion percentage vs. electrolysis time by Cu@Cu-1 modified electrode at (-1.50 V, -1.80 V and 2.10 V) vs. SCE. All experiments were conducted by means of (80 mL; 0.05 M Na_2SO_4 + 200 mg/L NO_3^{-}), 120 min, 25 ± 1℃.

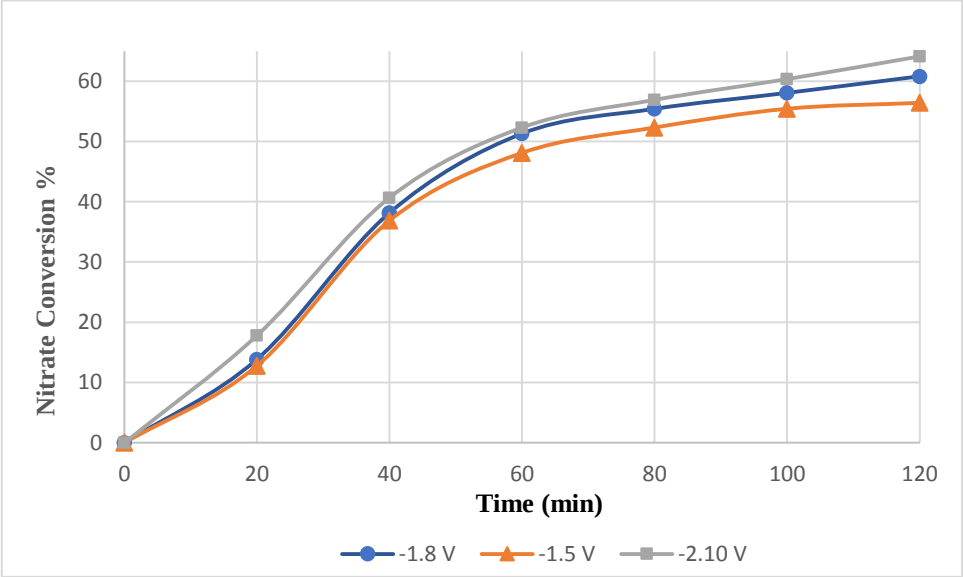

Figure A.9

*Nitrate conversion percentage vs. electrolysis time by Cu@Cu-1 modified electrode at (**15** ℃, **25** ℃, & **35** ℃). All experiments were conducted employing (80 mL; 0.05 M Na_2SO_4 + 200 mg/L NO_3^{-}), 120 min, -1.80 V vs SCE).*

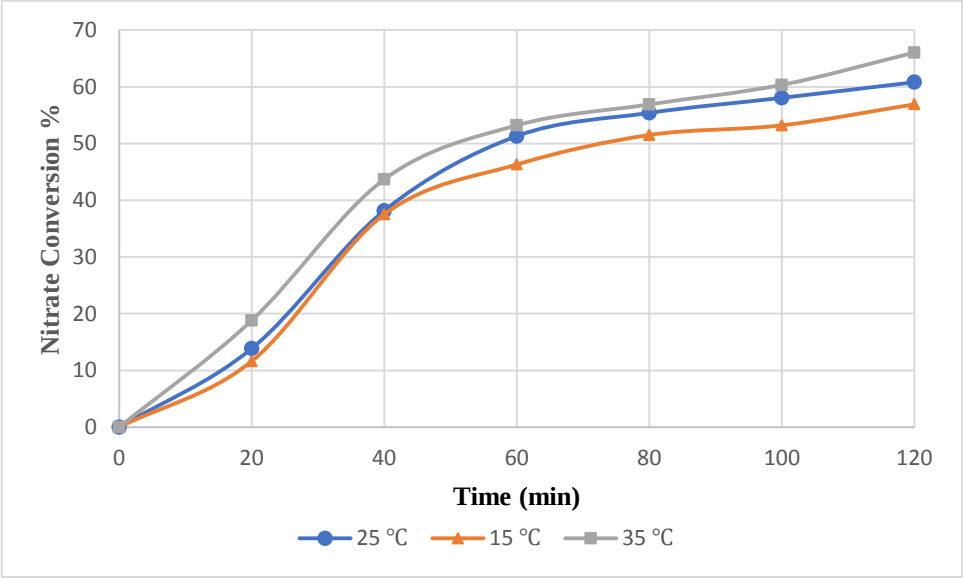

Figure A.10

Variation of pH throughout the 300 minutes of electrolysis. All experiments were conducted employing (80 mL; 0.05 M Na_2SO_4 + 200 mg/L NO_3^{-}), 120 min, -1.80 V vs SCE.

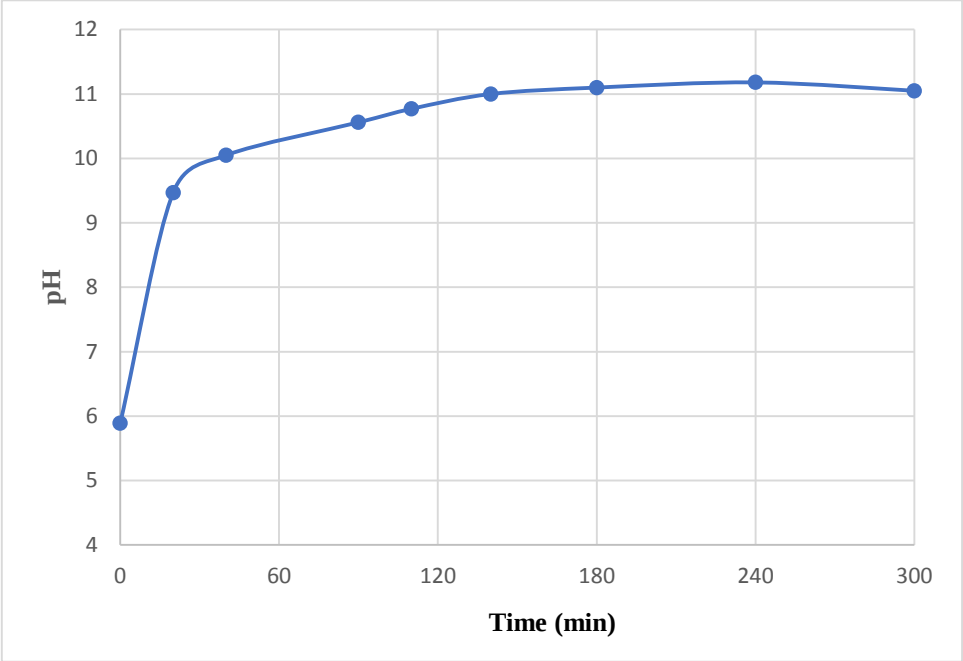

Figure A.11

Nitrate conversion percentage with different initial concentrations by Cu@Cu-1 electrode. All experiments were conducted employing (80 mL; 0.05 M Na_2SO_4 + 200, 600 and 800 mg/L NO_3^{-}), 120 min, -1.80 V vs SCE.

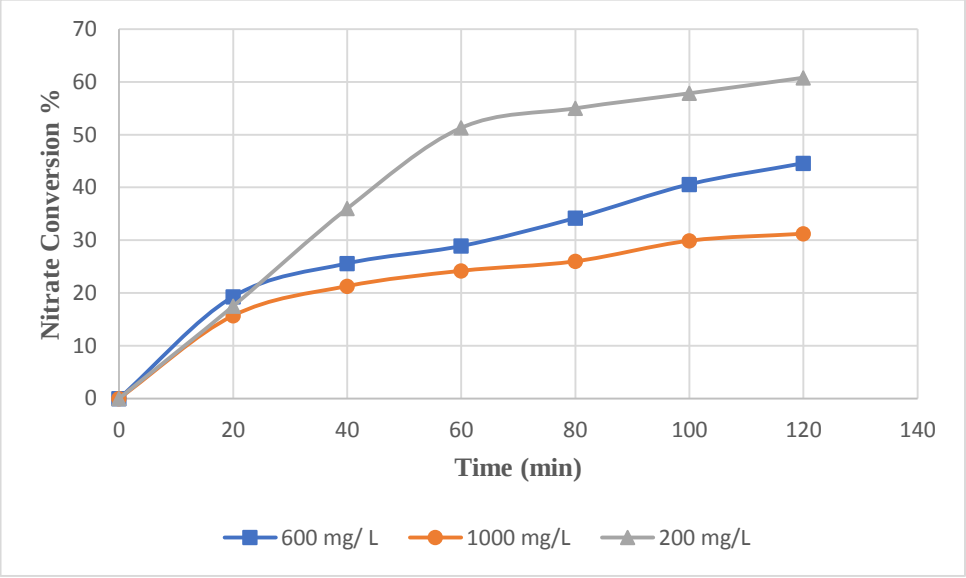

Figure A.12

Three separate two-hour trials measuring the nitrate conversion percentage with the same Cu@Cu-1 electrode. All experiments were conducted employing (80 mL; 0.05 M Na_2SO_4 + 200 mg/L NO_3^{-}), 120 min, -1.80 V vs SCE.

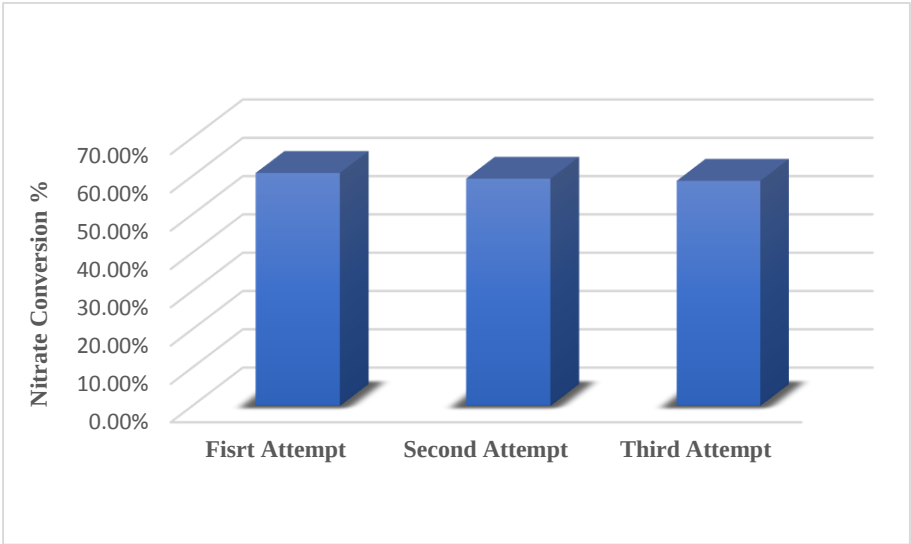

Figure A.13

Nitrate electroreduction kinetics per (a) Zero Oder Law, (b) First Order Law, & (c) Second Order Law by Cu@Cu-1 modified electrode. All experiments were conducted employing (80 mL; 0.05 M Na_2SO_4 + 200 mg/L NO_3^{-}), 120 min, -1.80 V vs SCE.

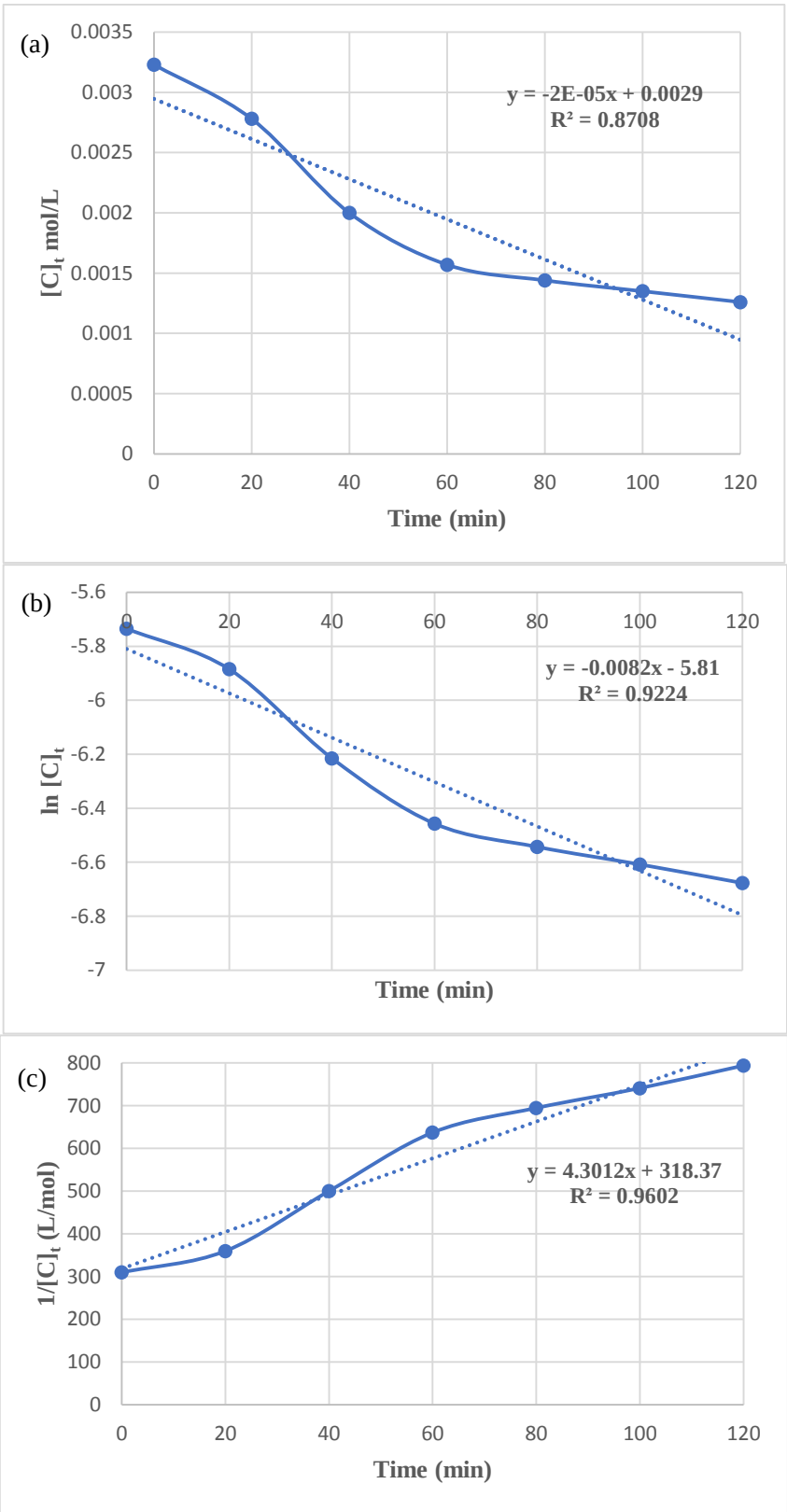

Figure A.14

Influence of the initial nitrate concentration on the initial rate of electroreduction by Cu@Cu-1 modified electrode. All experiments were conducted employing (80 mL; 0.05 M Na_2SO_4 + 200 mg/L NO_3^{-}), 120 min, -1.80 V vs SCE.

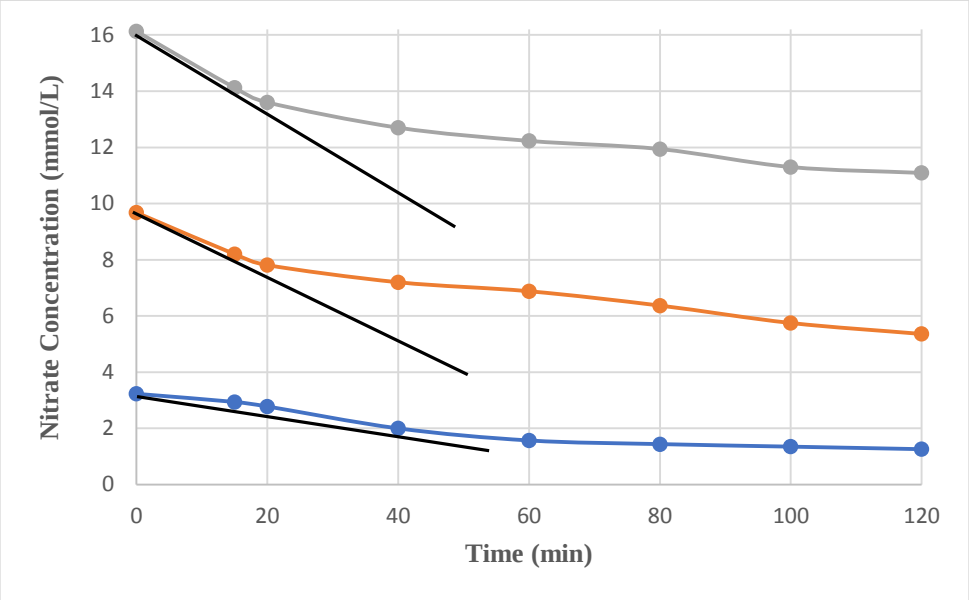

Figure A.15

ln $Rate_{initial}$ vs. ln $[C]_0$ plot by Cu@Cu-1 modified electrode. All experiments were conducted employing (80 mL; 0.05 M Na_2SO_4 + 200 mg/L NO_3^{-}), 120 min, -1.80 V vs SCE.

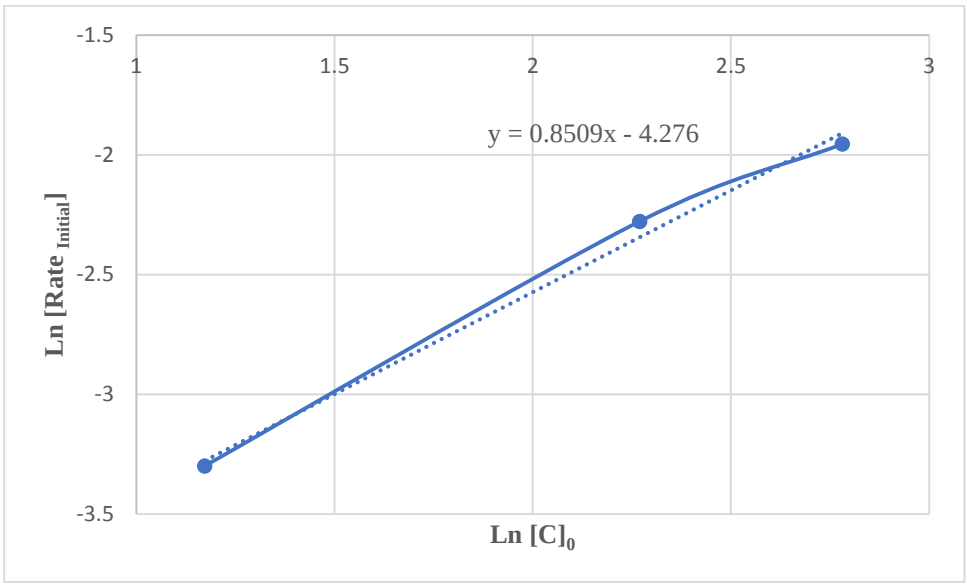

جامعة النجاح الوطنية
كلية الدراسات العليا

تحضير حبيبات النحاس النانوية على صفائح النحاس وتطبيقاتها كحفازات كهربائية في نزع النترات من الماء

إعداد
سماء مسعود أسعد حجازي

إشراف
أ. د. حكمت هلال
د. هبه نصار

قدمت هذه الرسالة استكمالا لمتطلبات الحصول على درجة الماجستير في الكيمياء،
من كلية الدراسات العليا، في جامعة النجاح الوطنية، نابلس – فلسطين.

2024

تحضير حبيبات النحاس النانوية على صفائح النحاس وتطبيقاتها كحفازات كهربائية في نزع النترات من الماء

إعداد

سماء مسعود أسعد حجازي

شراف

أ. د. حكمت هلال

د. هبه نصار

الملخص

تشكل مسألة تلوث المياه، وبالتحديد أيونات النترات، مصدر قلق متزايد على الصعيدين العالمي والفلسطيني. ويتعلق ذلك بكل من مصادر المياه الجوفية والمياه السطحية. ويمكن أن يعزى تصاعد التلوث المتعلق بالنترات إلى الاستخدام المفرط وغير السليم للمواد الكيميائية نتيجة للأنشطة البشرية. ويمثل استخدام الإختزال الكهروكيميائي للنترات طريقة صالحة لمعالجة هذه المسألة. والهدف الرئيسي من هذه الدراسة هو التخلص من ايون النترات في الماء عن طريق اختزاله خاصة الى غاز النيتروجين الامن. ويتحقق الهدف المذكور أعلاه من خلال تطوير اقطاب كهربائية غير مكلفة وآمنة وتحقق كفاءة استثنائية في الحد من النترات. واستُخدمت الخلية الكهروكيميائية غير المجزأة لإجراء الاختزال الكهروكيميائي للنترات المائية. وتألفت الخلية الكهروكيميائية غير المجزأة من ثلاثة أقطاب كهربائية: القطب المرجعي ويعرف ب (SCE)، والقطب المقابل كمصعد كان على هيئة صفيحة بلاتينوم (Platinum)، والمهبط كان من أحد الأقطاب المعدلة في هذا البحث. وقد تكونت الأقطاب المعدلة من عدة فئات. وتتكون الفئة الأولى من ذرات النحاس النانوية المترسبة على صفيحة نحاس من خلال الترسيب الكهربائي. وتتكون الفئة الثانية من الاقطاب النحاسية التي أنشأتها عملية النقش الكيميائي باستخدام مادة كلوريد الحديديك. وتشمل الفئة الثالثة صفيحة نحاس معدلة بالغرافين وقد أُلغي هذا التعديل لأسباب عدة ستناقش لاحقاً. وقد خضعت هذه الأقطاب للتصنيف و التحليل من خلال استخدام حيود الأشعة السينية (XRD)، والمسح الجهري الالكتروني (SEM)، التحليل الطيفي المشتت لطاقة العناصر (EDS)، التحليل الطيفي المشتت للأشعة السينية(XPS) . تم بعد ذلك فحص الاختزال الكهروكيميائي للنترات من خلال الأقطاب المعدلة، المذكورة أعلاه. من بين الأقطاب المعدلة تم اختيار القطب المسمى ب (Cu@Cu-1) المعدل من خلال ترسيب ذرات

النحاس النانوية عن طريق الترسيب الكهربائي. وأظهرت النتائج ان هذا القطب اظهر اهم معدل تحويل نتـــرات حيث بلغت 92.3 بالمئة خلال إطار زمني مدته 120 دقيقة. وعلاوة على ذلك، أظهرت هـــذه العينـــة أفضـــل انتقائية لإنتاج النيتروجين، بمعدل 85.05 في المائة. وقد تحققت هذه النتائج في ظل ظروف حرارة معتدلة تبلغ (25 ± 1 درجة مئوية) وعند فرق جهد بلغ 1.80- فولت. لذلك تم تفضيل هذا القطب لإكمال بـــاقي اعمـــال الدراسة. وعلاوة على ذلك، تم فحص قانون السرعة لعملية الاختزال للنترات. وكشف التحقيق عن معـــدل رد فعل يبلغ 0.85، مصحوباً بمعدل ثابت قدره $1.39 \times 10^{-2}\ min^{-1}$.

الكلمات المفتاحية: النحاس، ذرات النحاس النانوية، النترات، التلوث المائي، الاختزال الكهروكيميائي.